Check for updates

View Article Online
View Journal

Journal of
Materials Chemistry B

Materials for biology and medicine

Accepted Manuscript

This article can be cited before page numbers have been issued, to do this please use: Z. Xiang, L. Yang, B. Yu, Q. Zeng, T. Huang, S. Shi, H. Yu, Y. Zhang, J. Wu and M. Zhu, *J. Mater. Chem. B*, 2024, DOI: 10.1039/D4TB02090A.

This is an Accepted Manuscript, which has been through the Royal Society of Chemistry peer review process and has been accepted for publication.

Accepted Manuscripts are published online shortly after acceptance, before technical editing, formatting and proof reading. Using this free service, authors can make their results available to the community, in citable form, before we publish the edited article. We will replace this Accepted Manuscript with the edited and formatted Advance Article as soon as it is available.

You can find more information about Accepted Manuscripts in the Information for Authors.

Please note that technical editing may introduce minor changes to the text and/or graphics, which may alter content. The journal's standard Terms & Conditions and the Ethical guidelines still apply. In no event shall the Royal Society of Chemistry be held responsible for any errors or omissions in this Accepted Manuscript or any consequences arising from the use of any information it contains.

ROYAL SOCIETY OF CHEMISTRY

rsc.li/materials-b

View Article Online
DOI: 10.1039/D4TB02090A

Recent Advances in Polymer-based Thin-film Electrode for ECoG Applications

Zhengchen Xiang, Liangtao Yang, Bin Yu*, Qi Zeng, Tao Huang, Shuo Shi, Hao Yu, Yi Zhang*, Jinglong Wu, Meifang Zhu*

Z. Xiang, B. Yu, T. Huang, Prof. H. Yu, Prof. M. Zhu
State Key Lab for Modification of Chemical Fibers and Polymer Materials, College of Material Science and Engineering, Donghua University, Shanghai 201620, China

E-mail: yubin@dhu.edu.cn (B. Yu)

L. Yang, Q. Zeng, Y. Zhang, Prof. J. Wu
Research Center for Medical Artificial Intelligence, Shenzhen Institute of Advanced Technology, Chinese Academy of Sciences, 518055 Shenzhen, China

E-mail: liangtao.yang@siat.ac.cn (L. Yang), yi.zhang3@siat.ac.cn(Y. Zhang)

S. Shi
School of Fashion and Textiles, The Hong Kong Polytechnic University, 999077, Hong Kong S.A.R, China

Keywords: brain-computer interface, polymer materials, ECoG thin-film electrode, biopotential

Open Access Article. Published on 12 November 2024. Downloaded on 11/23/2024 4:14:03 AM.
This article is licensed under a Creative Commons Attribution 3.0 Unported Licence.

Journal of Materials Chemistry B Accepted Manuscript

Abstract

Electrocorticography (ECoG) has garnered widespread attention due to its superior signal resolution compared to conventional electroencephalogram (EEG). While ECoG signal acquisition entails invasiveness, the invasive rigid electrode inevitably inflicts damage on brain tissue. Polymer electrodes that combine conductivity and transparency have garnered great interest, due to that they not only facilitate high-quality signal acquisition but also provide additional insights while preserving the health of the brain, positioning them as the future frontier in the brain-computer interface (BCI). This review summarizes the multifaceted functions of

View Article Online
DOI: 10.1039/D4TB02090A

polymers in ECoG thin-film electrode for BCI. We present the abilities of sensitive and structural polymers focusing on the impedance reduce, signal quality improvement, good flexibility, and transparency. Typically, two sensitive polymers and four structural polymers are detailed analyzed in properties for ECoG electrode. Moreover, the underlying mechanism of polymer-based electrode in signal quality enhancement are also revealed. Finally, the remaining challenges and perspectives are also discussed.

Open Access Article. Published on 12 November 2024. Downloaded on 11/23/2024 4:14:03 AM.
This article is licensed under a Creative Commons Attribution 3.0 Unported Licence.

Journal of Materials Chemistry B Accepted Manuscript

View Article Online
DOI: 10.1039/D4TB02090A

Open Access Article. Published on 12 November 2024. Downloaded on 11/23/2024 4:14:03 AM.
This article is licensed under a Creative Commons Attribution 3.0 Unported Licence.

Journal of Materials Chemistry B Accepted Manuscript

1. Introduction

Brain-computer interface (BCI) is the technology that transmits biopotential signals generated by stimulating neurons in the brain to external electronic devices, enabling artificial control and intervention[1, 2, 3]. Electrocorticography (ECoG) is obtained through the thin film electrodes on the skull of brain, resulting in higher electrical signal intensity than Electroencephalogram (EEG) that is recorded on the scalp invasively. Both of them are highly suitable for BCI application to monitor health status.[4, 5, 6, 7] Additionally, BCI has also been employed for drug delivery[8, 9] through the implantation of microchannel electrodes, offering treatments for neurological disorders, such as epilepsy, Alzheimer's disease, and Parkinson's disease[10]. These advances in BCI technology possess great promise for neural healthcare management and artificial intelligence.[11]

To meet the demands of BCI development, it is crucial to record stable and high-quality biopotential signals, which has led to increased attention on electrodes.[12, 13] The electrodes for the brain potential recording can be categorized into non-invasive, semi-invasive, and invasive electrodes. Non-invasive electrodes are always used to monitor brain alpha and beta rhythms (0~40 Hz) through external monitoring, completely avoiding interference with brain tissue. Performance distinctions among three different types of electrodes exhibiting varying degrees of invasiveness are outlined in **Table 1**, and the differentiation between these diverse signals is listed in **Table 2**.[14] However, non-invasive electrodes are strongly affected by the skull, and the signal quality of them may not meet the requirements for deeper-level research. The

View Article Online
DOI: 10.1039/D4TB02090A

Open Access Article. Published on 12 November 2024. Downloaded on 11/23/2024 4:14:03 AM.
This article is licensed under a Creative Commons Attribution 3.0 Unported Licence.

Journal of Materials Chemistry B Accepted Manuscript

invasive electrodes penetrate into the brain to obtain high-resolution biopotential signals, like local field potential (LFP) and action potential (AP). However, these invasive electrodes are made of rigid materials like steel, which is not flexible for brain tissue.[15] This leads to tissue damage during experiments, limiting subject mobility. Moreover, long-term implantation of probes leads to the accumulation of glial sheaths around the probe,[1, 16, 17, 18, 19, 20] reducing the electrode's stability.[21, 22] Semi-invasive electrodes especially ECoG electrodes primarily consist of two-dimensional thin-film. These thin-film electrodes are typically placed under the hard meninges on the surface of the cerebral cortex and can record ECoG signals with high bandwidth and low noise.[23] These collected good signals contribute to the study of BCI. Due to the good elastic properties of thin-film materials, electrode implantation causes minimal interference to brain tissue, making it a subject of interest. In recent years, research on semi-invasive electrodes has attracted great attention.[24, 25] The recent development of ECoG thin-film electrodes is shown in **Figure 1**.

Table 1. Comparison of three different types of electrodes in skull filtration, craniotomy, and nerve injury.

Type	Skull filtration	Craniotomy	Nerve injury	Ref
Non-invasive	Yes	None	None	[26]
Semi-invasive	No	Craniotomy	None	[25]
Invasive	No	Craniotomy	Nerve injury	[27, 28]

View Article Online
DOI: 10.1039/D4TB02090A

Table 2. Neural signal comparison[14]

Sign	Frequency	Amplitude	Rhythm	Stability
EEG	0.5~100 Hz	5~300 μV	Slow rhythms	Decades
ECoG	< 200 Hz	0.01~5 mV	Medium rhythms	Decades
LFP	< 200 Hz	0.01~1 mV	—	Year
AP	0.1~7 kHz	500 μV	—	Month

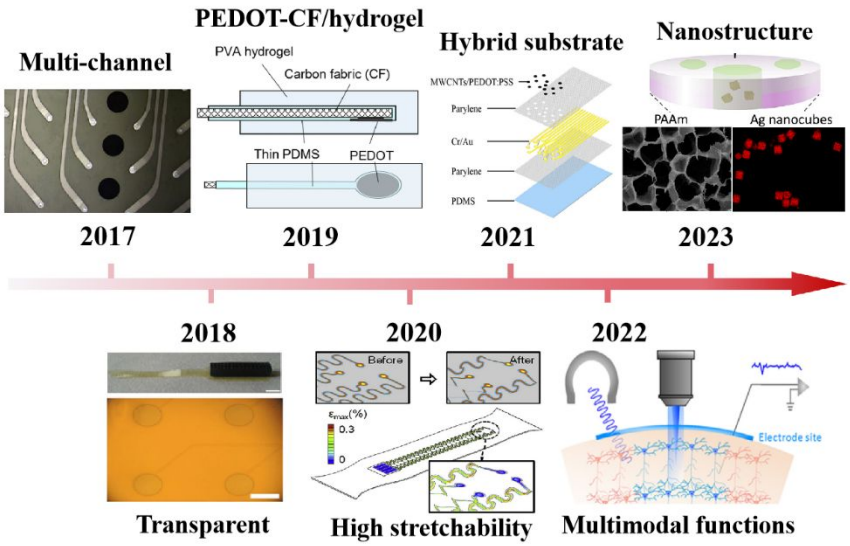

Figure 1. (a) Development of ECoG thin-film electrodes. Reprinted with permission from [29]. Copyright 2023, American Chemical Society. Reprinted with permission from [30]. Copyright 2022, Elsevier. Reprinted with permission from [31]. Copyright 2021, American Chemical Society. Reprinted with permission from [32]. Copyright 2020, Journal of Materiomics. Reprinted with permission from [33]. Copyright 2019, Scientific Reports. Reprinted with permission from [34]. Copyright 2018, Elsevier. Reprinted with permission from [35]. Copyright 2017, Elsevier.

Open Access Article. Published on 12 November 2024. Downloaded on 11/23/2024 4:14:03 AM.
This article is licensed under a Creative Commons Attribution 3.0 Unported Licence.

Journal of Materials Chemistry B Accepted Manuscript

View Article Online
DOI: 10.1039/D4TB02090A

Open Access Article. Published on 12 November 2024. Downloaded on 11/23/2024 4:14:03 AM.
This article is licensed under a Creative Commons Attribution 3.0 Unported Licence.

Journal of Materials Chemistry B Accepted Manuscript

The configuration of semi-invasive electrodes requires good shape contact with the brain. However, traditional ECoG electrodes, due to the rigidity of silicon-based substrates and metal conductors, mismatch the request on the mechanical properties of brain tissue.[36] Polymer materials provide an excellent solution to avoid this mechanical mismatch. Conventional polymer materials have a low Young's modulus; for example, polydimethylsiloxane (PDMS)[31, 37, 38, 39, 40, 41, 42, 43] , polyimide (PI)[44] and parylene[31, 32, 38, 40, 43, 45, 46, 47, 48, 49, 50, 51, 52, 53, 54, 55]. Some studies have achieved both high tensile strength and good transparency by using a combination of two polymer films. This opens up possibilities for further application of ECoG electrodes in optogenetics, providing the potential for external control of the brain. PI can be used to form flexible films for circuit integration and active electronic devices through spin coating and electrospinning.[56, 57] Liquid crystal polymer (LCP) has also received more attention due to its excellent biocompatibility.[58, 59, 60] Furthermore, to improve the conformal contact between the electrode and brain tissue, conductive polymers are typically coated on the surface of a metal layer. These polymer materials reduce the contact impedance between electrode and skin interface, due to their good conductivity and flexibility compared to metal materials. Poly(3,4-ethylenedioxythiophene):poly(styrene sulfonate) (PEDOT:PSS) have high transparency and good conductivity, these properties make this material widely used in the preparation of electrophysiological electrodes. Sergio et al. introduced PEDOT:PSS into Pt electrodes by electroplating, leading to the lower electrochemical impedance by

View Article Online
DOI: 10.1039/D4TB02090A

approximately 30 times (from 971007 Ω to 30407.6 Ω) at 1 kHz compared to the bare Pt electrode. Polymer can significantly improve the signal quality of ECoG, it has become one of the most critical electrode components for brain biopotential recording.

With the growing interest in BCI, more and more articles are being published on the understanding of this interdisciplinary field.[11] In terms of engineering, there is a focus on achieving more extensive and long-term recordings.[61] These reports focused on the development, prospects, and application scenarios of BCIs.[62] In terms of materials science, conductive materials such as silicon-based materials[63], fiber materials[64], conjugated polymer materials[65], and semiconductor polymer materials[66] have been reviewed and discussed. However, most of these reviews introduced the electrodes only by their physiochemical properties. There is still lack a comprehensive discussion about the correlation between the structure, properties and signal performance.

In this work, the electrode performance was classified based on the detection requirements of ECoG signals, including electrical properties, mechanical properties, and optical properties. The criteria to be considered mainly include electrode-skin impedance, Young's modulus, and transparency, are summarized. According to our investigation, the addition of polymer materials has brought improvements to ECoG thin-film electrodes in terms of conductivity and flexibility, demonstrating the potential for enhancing electrode signal quality. In order to clearly distinguish these polymer materials, they are divided into two categories based on their contribution to electrode properties. The one is sensitive materials, like PEDOT and PPy were contact with skin

Open Access Article. Published on 12 November 2024. Downloaded on 11/23/2024 4:14:03 AM.
This article is licensed under a Creative Commons Attribution 3.0 Unported Licence.

Journal of Materials Chemistry B Accepted Manuscript

View Article Online
DOI: 10.1039/D4TB02090A

because of their high conductivity. The other is structure materials, like polydimethylsiloxane, parylene, polyimide, liquid crystal polymer etc. were commonly used for the substrate and insulation layer of ECoG thin-film electrode. the available electrode preparation methods and relevant properties are discussed. Finally, the challenges and perspectives of polymer-based ECoG thin-film electrodes are also discussed.

2. Characteristics of Polymer Materials

ECoG thin-film electrodes are divided into two parts: sensitive materials and structural materials. The sensitive materials provide the electrical properties required for the electrodes, while the structural materials like substrate, insulation layer and sacrificial layer provide the mechanical and optical properties required for the electrodes such as structural support, adhesion of metals, and improvement of transmittance.[12]

The electrode materials and thin-film materials for ECoG thin-film electrodes are compared in **Table 3**. The performance of electrodes with different materials, including sensitive materials of Ti, Au, Cr, Pt, indium tin oxide (ITO), poly(3,4-ethylenedioxythiophene)-modified carbon fabric (PEDOT-CF), PEDOT:PSS, multiwalled carbon nanotubes (MWCNTs), and structure materials of polyvinyl alcohol (PVA), PDMS, PI, and polyethylene glycol terephthalate (PET) are listed.

Open Access Article. Published on 12 November 2024. Downloaded on 11/23/2024 4:14:03 AM.
This article is licensed under a Creative Commons Attribution 3.0 Unported Licence.

Journal of Materials Chemistry B Accepted Manuscript

Open Access Article. Published on 12 November 2024. Downloaded on 11/23/2024 4:14:
This article is licensed under a Creative Commons Attribution 3.0 Unported

Table 3. The materials and properties of the ECoG thin-film electrodes.

	Sensitive materials	Structural materials	Property	Ref
1	Ti/Au	parylene C and PDMS	Bending cycle reaches 200000 times Impedance is 12.65 kΩ at 1 kHz charge storage capacity is 207.5 μCcm^{-2}	[38]
2	Ti/Au	parylene C	Impedance is 10^4 Ω level at 1 kHz Long-term recording stability	[51]
3	Au	PI	Impedance is 10^7 Ω level at 1 kHz max strain less than 0.03% at 3.8 mm bending radius	[67]
4	Au	PI	Impedance is 1.1 ± 1.2 kΩ at 1 kHz	[68]
5	Au	parylene and PDMS	Impedance between 50 and 70 kΩ at 1 kHz	[48]
6	Pt	OSTEMER 324 Flex	Surface curvature adapts to the brain	[69]

Journal of Materials Chemistry B Accepted Manuscript

Open Access Article. Published on 12 November 2024. Downloaded on 11/23/2024 4:14
This article is licensed under a Creative Commons Attribution 3.0 Unport

7	Cr/Au	BPDA-PD PI	Waterproofness	[70]
8	Cr/Au/Pt	parylene C	Transparent	[47]
9	Pt	PI 2611	Impedance is 10^2 Ω level at 1 kHz	[25]
10	Glassy Carbon	PI	Impedance is 10^4 Ω level at 1 kHz (300 μm)	[71]
11	Glassy Carbon	PI	Impedance is 10^4 Ω level at 1 kHz Long-term recording stability	[72]
12	ITO	parylene C and PDMS	Transparent	[52]
13	ITO	PI	Transparent	[34]
14	ITO	parylene HT	Transparent	[50]
15	Carbon nanotube array	PDMS	Transparent Extracellular ion monitoring	[41]
16	PEDOT-CF	PVA hydrogel and PDMS	Shape adaptability Double layer capacitance is 70 mF cm^{-2}	[33]

Journal of Materials Chemistry B Accepted Manuscript

Open Access Article. Published on 12 November 2024. Downloaded on 11/23/2024 4:14:
This article is licensed under a Creative Commons Attribution 3.0 Unported

17	PEDOT:Nafion coated gold	PI	|Z| values are about 100 kΩ at 1 kHz	[73]
18	PEDOT:PSS–ITO–Ag–ITO	parylene C	Young's modulus is about 4.064 GPa The resistivity of the average thin layer resistance is 7.40×10^{-5} Ω cm Transparent	[49]
19	(MWCNTs)/ PEDOT:PSS	PDMS–parylene hybrid	Average Impedance is 20.2 ± 7.9 kΩ at 1 kHz Transparent	[31]
20	Silver and PEDOT:PSS	PET and parylene	Impedance is 81.4 ± 53.4 kΩ at 1 kHz Transparent	[74]
21	Cr/Au/Ti coated PEDOT-CNT	PI	Impedance is 10^3 Ω level at 1 kHz	[75]
22	PEDOT:PSS coated Pt/Au/Pt	parylene C and PDMS	Impedance is 30.4 ± 2.4 kΩ at 1 kHz Transparent	[43]

Journal of Materials Chemistry B Accepted Manuscript

View Article Online
DOI: 10.1039/D4TB02090A

Open Access Article. Published on 12 November 2024. Downloaded on 11/23/2024 4:14:03 AM.
This article is licensed under a Creative Commons Attribution 3.0 Unported Licence.

Journal of Materials Chemistry B Accepted Manuscript

2.1 Electrical properties

Acquiring ECoG signals necessitates electrode materials possessing favorable electrical characteristics. For polymer materials, conductive polymers (CPs)[76] with lower impedance are often used for electrodes. These CPs encompass organic polymeric conductors, such as PEDOT, polypyrrole (PPy), and polyaniline (PANI)[77, 78]. PPy is a biocompatible substance extensively employed in biomedical scenarios, and it can be synthesized via chemical oxidation, electrochemical oxidation, and photopolymerization methods.[79] PANI offers the advantages of cost-effectiveness and ease of synthesis. Nevertheless, the primary polymer chain's rigidity renders to engage in machining operations.[80, 81] PEDOT exhibits the advantages of good suppleness, high transparency, and good conductivity.[82] Incorporating PSS into PEDOT yields water-soluble PEDOT:PSS, thereby enhancing its processing performance.[83, 84]

CPs can be modified onto the electrode surface via coating or electroplating methods, with the intention of mitigating electrode impedance. Sergio et al. employed electroplating to coat PEDOT:PSS onto the Pt electrode, reducing the electrochemical impedance by 30 fold.[43] **Figure 2a** illustrates the contact impedance of PANI-coated electrodes and bare electrodes. The PANI coating leads to a reduction in electrode contact impedance ($Z = 120\ \Omega\ cm^2$ vs. $Z = 1808\ \Omega\ cm^2$).[85] Similarly, the same trend is observed with PPy coating. Rikky et al. compared the impedance of PPy+FOS (blue) with those of gold (red), unveiling a decrease in electrode impedance following PPy coating (Figure 2b).[8] Saeed et al. enhanced the conductivity from 10^{-4} to 10^{-2} by introducing oligoaniline into the composition.[86] Yang et al. designed and added

View Article Online
DOI: 10.1039/D4TB02090A

PEDOT:PSS on the surface of ITO-Ag-ITO structure, which greatly reduced the electrode impedance.[49] Moreover, the PEDOT:PSS coating further decreases the impedance. Castagnola et al. shows that the impedance Gold-CNT-coated electrode impedance diminished by two-thirds compared to the bared sample， and PEDOT-CNT-coated electrode achieved a two-order decrease in impedance at 100 Hz compared to the uncoated electrode.[87] Moreover, the electrical performance of the electrode is related to its size, as the electrode diameter decreases, the background noise within the acquired signal exhibits a concurrent rise (Figure 2c). However, small-sized ECoG electrodes are crucial for conducting experiments and maintaining better electrical property of ECoG electrodes at small sizes has become a challenge. Enhancing the material's electrical conductivity offers the mean to reduction of background noise. [71] Following the application of PEDOT:PSS coating onto a glassy carbon (GC) electrode with a 50 μm thickness, a background noise intensity is similar to a 300 μm diameter electrode can be achieved. This consequently mitigates the noise stemming from the reduction in electrode area.

Open Access Article. Published on 12 November 2024. Downloaded on 11/23/2024 4:14:03 AM.
This article is licensed under a Creative Commons Attribution 3.0 Unported Licence.

Journal of Materials Chemistry B Accepted Manuscript

View Article Online
DOI: 10.1039/D4TB02090A

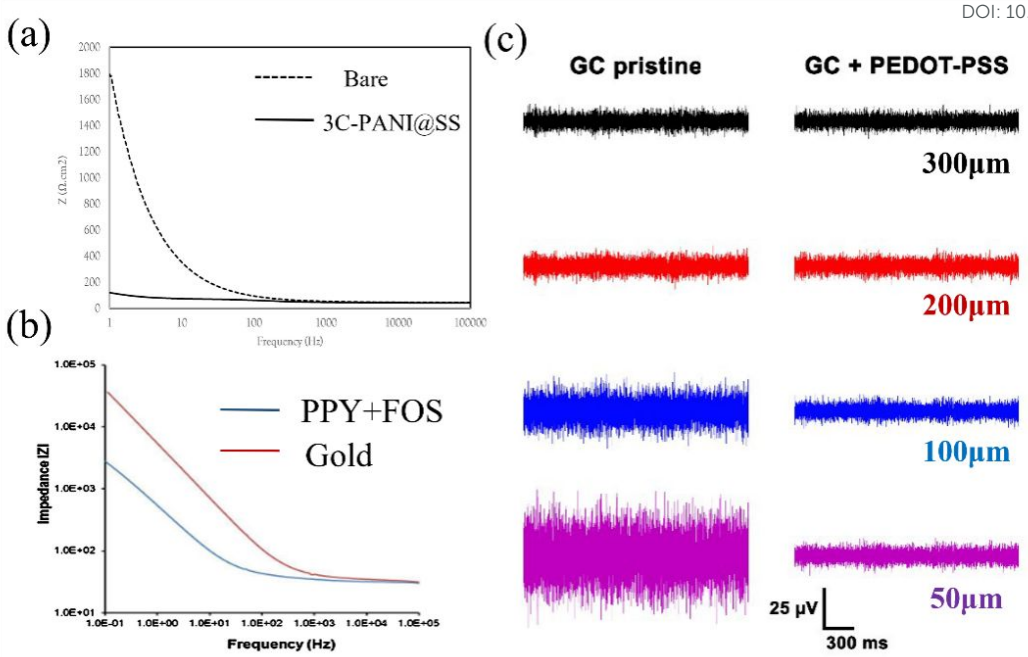

Figure 2. (a) The contact impedance between PANI coated electrode and bare electrode. Reprinted with permission from [85] Copyright 2021, Elsevier. (b) Impedance diagram between PPy coated electrode and bare electrode. Reprinted with permission from [8] Copyright 2016, Elsevier. (c) The electrode noise effects of GC electrodes with different areas with PEDOT:PSS. Reprinted with permission from [71] Copyright 2018, MDPI.

2.2 Mechanical properties

The mechanical properties of the electrode are determined by its Young's modulus.[88, 89] Polymer materials exhibit a similarity to brain tissue in terms of Young's modulus, distinguishing them from metal and non-metallic carbon-based materials (**Figure 3**). The reported flexible substrate materials for electrodes include PI, PDMS, parylene, and LCP. These materials enable the electrode to achieve good flexibility and stretchability, resulting in improved comfort and good contact to the skin and underlying tissue. As a result of this increased flexibility, the electrode achieves

Open Access Article. Published on 12 November 2024. Downloaded on 11/23/2024 4:14:03 AM.
This article is licensed under a Creative Commons Attribution 3.0 Unported Licence.

Journal of Materials Chemistry B Accepted Manuscript

View Article Online
DOI: 10.1039/D4TB02090A

improved accuracy and stability in acquiring ECoG signals.

Wu et al. mentioned that the modulus of brain tissue is about 100KPa, and the implantable Si electrode is about 150 GPa, this big mismatch will cause mechanical trauma, resulting in acute inflammation. They also measured the modules of hydrogels: ~100 kPa, Au: ~80 GPa, CNT: ~1 TPa. Wang et al. reported that the modulus of white mater and grey matter is about 300 Pa and 450 Pa，and dura mater is about 1 MPa. Guo et al. demonstrated the Young's modulus of different soft film materials (PDMS: ~1 MPa, PI: ~2.8 GPa, parylene: ~4.5 GPa, SU-8: ~5.6 GPa). Yang et al.claimed that the modulus of LCP is from MPa to GPa level. From the perspective of mechanical properties, hydrogel seems to be the most suitable material, but it is seriously affected by the moisture condition and has high requirements for the use environment.

In many cases, PDMS and LCP emerge as more flexible options for a wide range of microfluidic applications and biomedical devices. Their flexibility and biocompatibility render them preferable choices. Conversely, in settings necessitating printed circuits or stringent conditions, PI stands out as an excellent option due to its high temperature stability and chemical inertness, enabling optimal performance even under extreme circumstances. Moreover, parylene demonstrates proficiency in bonding with sensitive materials. Its highly uniform coating and good chemical inertness establish it as a frequently utilized protective coating in both biomedical and electronic devices.

Open Access Article. Published on 12 November 2024. Downloaded on 11/23/2024 4:14:03 AM.
This article is licensed under a Creative Commons Attribution 3.0 Unported Licence.

Journal of Materials Chemistry B Accepted Manuscript

View Article Online
DOI: 10.1039/D4TB02090A

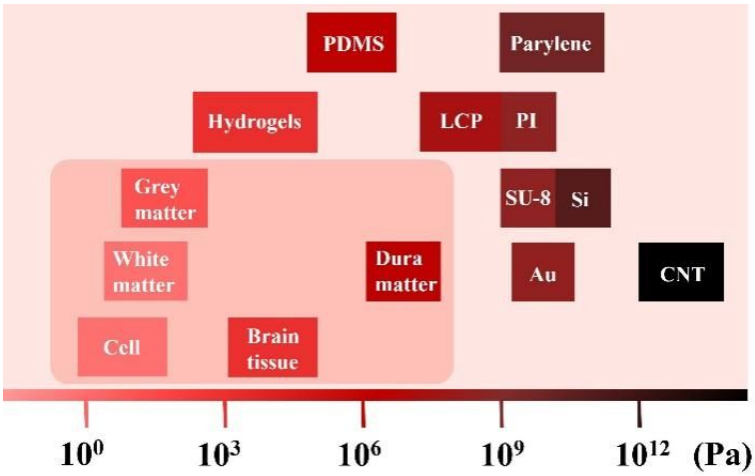

Figure 3. The Young's modulus of various materials, cell and brain tissue (scale bar). Data derived from [1, 30, 42, 58].

2.3 Optical properties

In contrast to many metal and inorganic non-metallic counterparts, polymer materials typically exhibit superior light transmittance. This is beneficial for stimulating the brain with light to achieve disease treatment. The schematic diagram of light stimulation is shown in **Figure 4a**. Figure 4b shows an ECoG thin-film electrode made of various polymer materials, which has good transparency.[30] For example, optogenetics affords targeted neuronal manipulation with millisecond precision,[90] enabling the potential artificial regulation of brain nerve excitation through light stimulation for addressing neurodegenerative disorders, i.e. Parkinson's disease, epilepsy, and depression.[91] Facilitated by highly light-transmissive ECoG electrodes, researchers employed optogenetics to modulate channel protein activity within the mouse brain, thus controlling nerve excitation and inhibition. Therefore, in recent years, there has been a growing research on the application of transparent polymer materials

Open Access Article. Published on 12 November 2024. Downloaded on 11/23/2024 4:14:03 AM.
This article is licensed under a Creative Commons Attribution 3.0 Unported Licence.

Journal of Materials Chemistry B Accepted Manuscript

View Article Online
DOI: 10.1039/D4TB02090A

in ECoG electrodes.[92]

Concerning optical properties, glass is commonly used as an inorganic transparent material for comparison, and indium-doped tin oxide (ITO) constitutes a commonly used transparent thin-film material.[93] Yang et al. conducted a comparison of transmittance between ITO and PEDOT:PSS-ITO-Ag-ITO multilayer films on glass and parylene C substrates. They noted an increase in transmittance on parylene C substrates from 78% (ITO) to 85% (multilayered film). Similarly, on glass substrates, the transmittance rises from roughly 75% (ITO) to about 89% (multilayered film). The study validated that the parylene C multilayered film achieves transmittance at wavelengths of 470 nm, 550 nm, and 630 nm.[46] Similarly, the electrode coated with PEDOT: PSS by Yang et al. showed stable signal-to-noise ratio (SNR) under different wavelengths of light conditions, with a variation of less than 2.7%, and an average signal-to-noise ratio range of 35db to 36db.With the successful preparation of transmittance ECoG electrode for more wavelengths of light, more choices can be obtained from light therapy to light stimulation. [47] Similarly, changes in the intensity of ECoG signals can also be used to detect the health status of the brain. Figure 4c displays the ECoG signals obtained by stimulating the marmoset brain with blue light. These signals were recorded using a 12-channel electrode. When the brain is affected by a virus, a high response is obtained through blue light stimulation, corresponding to the highest peak values of 150 μV in channels 1, 5, and 9 in Figure 4c, which correspond to the virus-infected area. This method of detecting signals through transparent electrodes to obtain health status is very useful for medical diagnosis. [49] Of course, it's

Open Access Article. Published on 12 November 2024. Downloaded on 11/23/2024 4:14:03 AM.
This article is licensed under a Creative Commons Attribution 3.0 Unported Licence.

Journal of Materials Chemistry B Accepted Manuscript

View Article Online
DOI: 10.1039/D4TB02090A

important to note that the duration of light stimulation and irradiance levels will also impact the photogenetically evoked potential, as they directly influence the activation and response of photosensitive cells or molecules, thus affecting the magnitude and duration of the elicited neural activity.

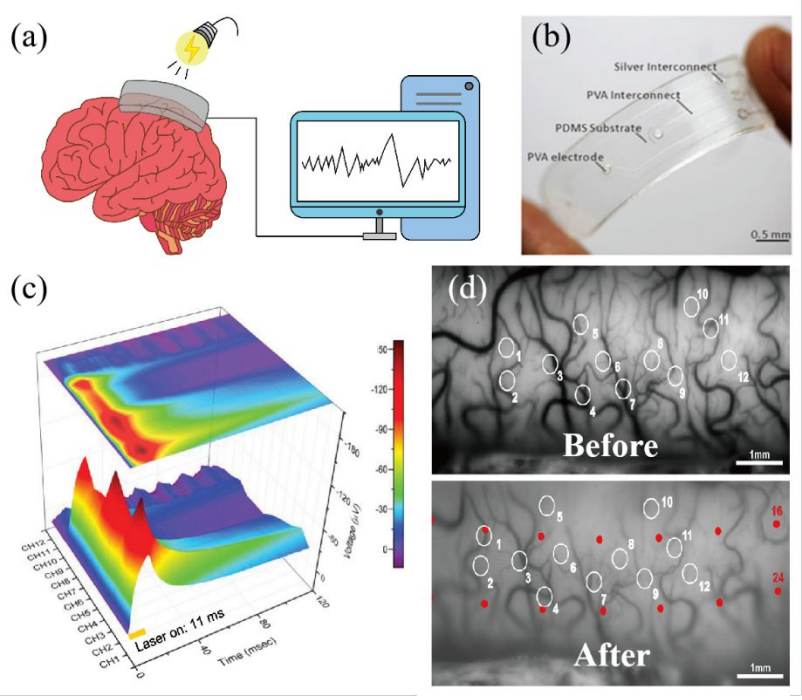

Figure 4. (a) The transparent ECoG thin-film electrode composed of multiple polymers. (b) Schematic diagram of ECoG signal stimulated by light. Reprinted with permission from [30] Copyright 2022, Elsevier. (c) The ECoG signal induced by continuous stimulation of the cerebral cortex of marmoset by a blue laser pulse through a transparent electrode for 11 milliseconds. Reprinted with permission from [94] Copyright 2019, WILEY (d) Vascular images of cat visual cortex A18 before and after the installation of the ECoG thin-film electrode. Reprinted with permission from [34] Copyright 2018, Elsevier.

3. Polymers for ECoG Thin-film Electrodes

In the following section, the materials are categorized as Sensitive materials and

Open Access Article. Published on 12 November 2024. Downloaded on 11/23/2024 4:14:03 AM.
This article is licensed under a Creative Commons Attribution 3.0 Unported Licence.

Journal of Materials Chemistry B Accepted Manuscript

View Article Online
DOI: 10.1039/D4TB02090A

Structure materials. For each specific material, we will first introduce their preparation methods, following by their properties.

3.1 Sensitive materials

Conductive polymers (CPs) predominantly derive their structure from a sequence of alternating single and double bonds. This conjugated arrangement facilitates the facile movement of electrons within and between polymer chains, thereby elevating the conductivity of polymer materials.[9] Notable instances include PANI,[85, 86] PPy[95] and PEDOT[2, 31, 33, 39, 43, 46, 49, 68, 71, 74, 75, 87, 96, 97, 98, 99]. CPs typically exhibit flexibility, conductivity, biocompatibility, and facile processing at ambient temperatures. The techniques employed for the deposition of CPs onto electrodes primarily involve spin coating and electropolymerization.[100] While spin coating technology is relatively straightforward, it is unsuitable for application on small, non-planar surfaces. In contrast, the electro-polymerization method proves to be a more precise approach for applying CPs to surfaces that are incompatible with spin coating techniques.[97, 101] For thin-film electrodes used in ECoG, the prevailing choice of CPs materials predominantly centers around PEDOT and PPy.[75, 96, 97]

3.1.1 Poly(3,4-ethylenedioxythiophene)

PEDOT is synthesized from the monomer EDOT through processes involving chemical oxidation and electrochemical polymerization.[83, 102, 103] It boasts attributes such as a narrow bandgap, chemical stability, and charge mobility.[104] Typically, PEDOT is combined with acidic PSS[105] to form PEDOT:PSS, a conductive polymer

Open Access Article. Published on 12 November 2024. Downloaded on 11/23/2024 4:14:03 AM.
This article is licensed under a Creative Commons Attribution 3.0 Unported Licence.

Journal of Materials Chemistry B Accepted Manuscript

View Article Online
DOI: 10.1039/D4TB02090A

Open Access Article. Published on 12 November 2024. Downloaded on 11/23/2024 4:14:03 AM.
This article is licensed under a Creative Commons Attribution 3.0 Unported Licence.

Journal of Materials Chemistry B Accepted Manuscript

that exhibits conductivity and transparency. The resultant conductive polymer PEDOT:PSS is a printable conductor[74]. Furthermore, it demonstrates superior impedance characteristics compared to conventional metal electrodes, especially within the frequency range of brainwave activity (0.1 Hz ~ 1000 Hz). Due to its good chemical stability and biocompatibility, PEDOT:PSS is highly suitable for long-term implanted ECoG thin-film electrodes.

In terms of structure, the electrode employs electropolymerization to prepare a PEDOT layer at the base of the carbon fabric (CF) electrode is an effective way , as displayed in **Figure 5a**.[33] The reverse side of the electrode and the lead are insulated through a thin PDMS coating, while the outer layer is treated with a PVA hydrogel. This design ensures the electrode maintains conductivity while retaining a flexibility equivalent to living tissue. Carbon nanotubes (CNTs) exhibit mechanical strength and electrical properties. The amalgamation of carbon nanotubes with PEDOT, leading to PEDOT-CNTs, serves to enhance conductivity,[106, 107, 108] stability, and augment adhesion to the electrode surface. For instance, the nanocomposite electrode created by multiwalled carbon nanotubes (MWCNTs) in conjunction with PEDOT:PSS yields a rugged and porous surface via a network of interwoven nanostructures, as depicted in Figure 5b.[31] This configuration increases the electrochemical surface area and elevates electrode conductivity. Although high conductivity has been achieved, there is still a lack of stable testing *in-vivo* environment. The transparent electrode made by Donaldson et al. (as shown in Figure 5c) was tested for impedance at 15 and 103 days of implantation to reflect the stability of the electrode, and the SNR of this electrode

View Article Online
DOI: 10.1039/D4TB02090A

showed no significant difference before and after long-term storage. This electrode used transparent PEDOT:PSS as a replacement for silver interconnects within the transparency window, achieving electrodes with both good conductivity and transmissivity [74]

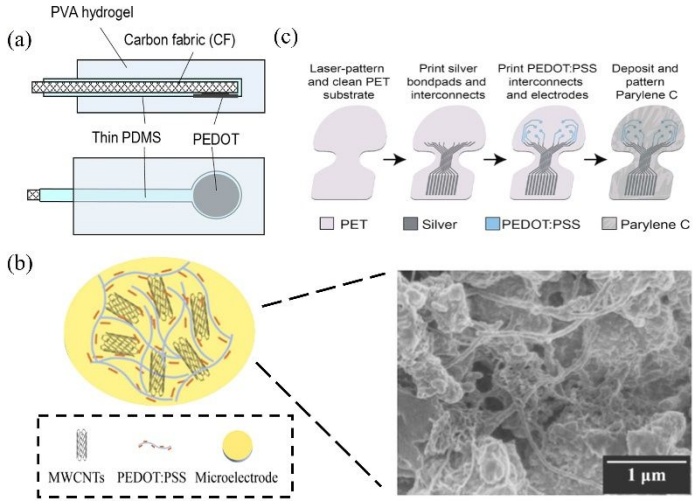

Figure 5. (a) Based on the cross section (top) and bottom view of the hydrogel PEDOT-CF ECoG electrode, the PEDOT-CF electrode has low impedance and is good to other conductive polymers in chemical stability and electrical performance. Reprinted with permission from [33] Copyright 2018, Scientific Reports. (b) Schematic representation of the electrochemical deposition of MWCNTs and PEDOT:PSS nanocomposites onto microelectrodes. The SEM image of the microelectrode structure is shown on the right. Reprinted with permission from [31] Copyright 2021, American Chemical Society. (c) A structural schematic diagram utilizes PET as a transparent patch material, enhancing the transparency of the electrode window. This improvement is achieved through the implementation of PEDOT:PSS interconnects in the window area, enabling contact with inkjet-printed silver interconnects. Reprinted with permission from [74] Copyright 2022, WILEY.

Open Access Article. Published on 12 November 2024. Downloaded on 11/23/2024 4:14:03 AM.
This article is licensed under a Creative Commons Attribution 3.0 Unported Licence.

Journal of Materials Chemistry B Accepted Manuscript

View Article Online
DOI: 10.1039/D4TB02090A

In terms of functionality, PEDOT exhibits good conductivity, transmittance, and biocompatibility, the schematic diagram of PEDOT deposition is shown in **Figure 6a**. As depicted in Figure 6b, it can be seen that when PEDOT-coated electrodes are implanted in the body (blue), there is a slight increase in impedance.[31] However, in comparison to the bare gold electrode (black), the impedance of the PEDOT-coated electrode experiences a significant decrease. Elisa et al. discovered that the application of PEDOT-CNT coating results in an expansion of the effective area of the electrode nanostructure, leading to an augmentation in the charge exchange between the electrode and the solution. They find that the integral area on the cyclic voltammetry (CV) curve magnifies by a factor of 350, and the enhancement in charge transfer capability becomes more pronounced as the size of the electrode being coated increases.[99] Additionally, the coating of PEDOT:PSS not only enhances electrical properties but also improves electrode optical properties. Yang et al. reveals that the effect of PEDOT:PSS coating, there is a slight increase in transmittance. This result makes PEDOT:PSS considered a polymer with advantages in preparing transparent electrodes.[49]

Open Access Article. Published on 12 November 2024. Downloaded on 11/23/2024 4:14:03 AM.
This article is licensed under a Creative Commons Attribution 3.0 Unported Licence.

Journal of Materials Chemistry B Accepted Manuscript

View Article Online
DOI: 10.1039/D4TB02090A

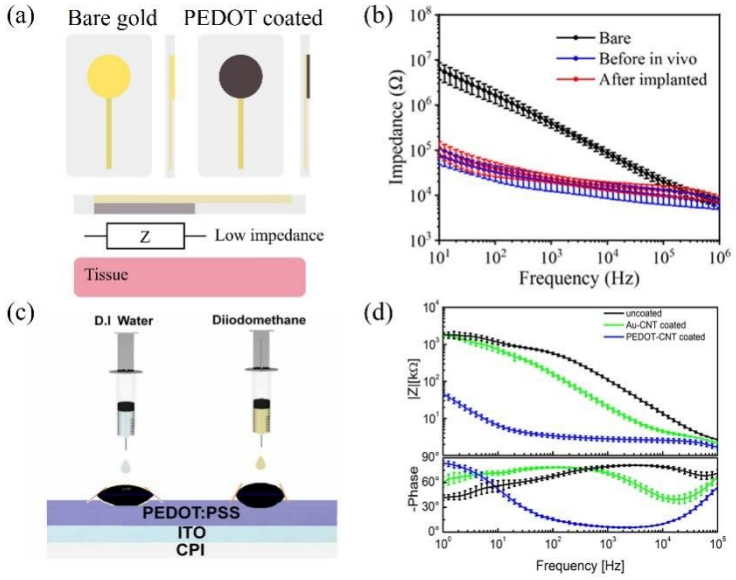

Figure 6. (a) Schematic diagram of electrodes before and after coating PEDOT. (b) Impedance comparison diagram related to bare (black), before in vivo (blue) and after implanted (red). Reprinted with permission from [31] Copyright 2021, American Chemical Society. (c) Measurement of the surface energy of the spin-coated PEDOT:PSS layer for the electrodes using D.I water and Diiodomethane. Reprinted with permission from [109] Copyright 2022, Elsevier. (d) Impedance spectra of uncoated (black), gold-CNT-coated (green), and PEDOT-CNT-coated (blue) electrodes (mean and standard deviation of 64 recording sites for each coating). Reprinted with permission from [87] Copyright 2013, American Chemical Society.

3.1.2 Polypyrrole

PPy is a common conductive polymer. Research on PPy began in 1989, Machida et al. synthesized highly conductive PPy with a conductivity of up to 190 S cm^{-1} in a ferric chloride solution. They found that when $FeCl_2$ was added before the reaction to control the oxidation potential of $FeCl_3$ in methanol solution, the conductivity of PPy could be increased to a value equivalent to that obtained through electrochemical

Open Access Article. Published on 12 November 2024. Downloaded on 11/23/2024 4:14:03 AM.
This article is licensed under a Creative Commons Attribution 3.0 Unported Licence.

Journal of Materials Chemistry B Accepted Manuscript

View Article Online
DOI: 10.1039/D4TB02090A

polymerization (220 S cm^{-1}).[110] This opens up a pathway for the chemical synthesis of highly conductive PPy, providing more options for subsequent work. For example, the electrode prepared by Qi et al. consists of a PDMS layer, a PPy layer, and PPy nanowires, where the PPy layer is electrochemically polymerized onto the PDMS layer (**Figure 7a**), to avoid the delamination of PPy electrode from the PDMS due to their mismatch in Young's modulus, they fabricated a layer of PPy nanowires on the PPy electrode to enhance their adhesion to skin, comparison of adhesion between before and after modification in Figure 7b. Rikky et al. fabricate a PPy electrode as a control system to release drug and monitor ECoG signal (Figure 7c).[8]

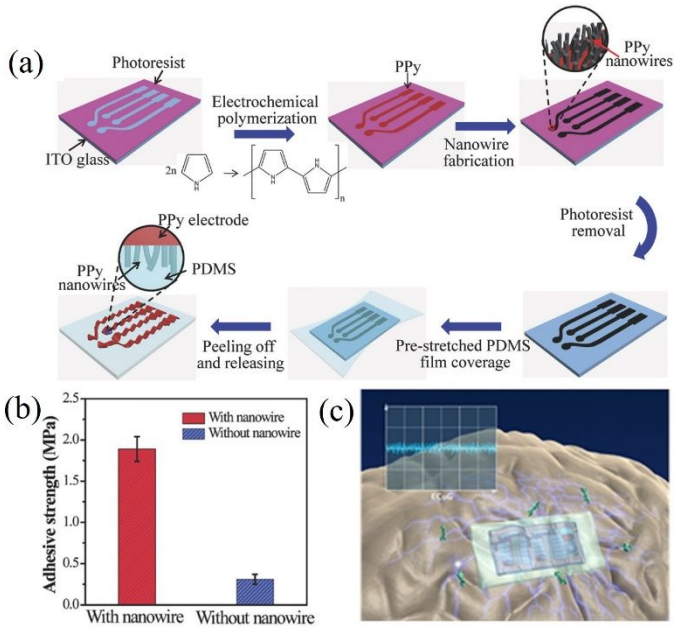

Figure 7. (a) A preparation method for PPy array electrodes. Reprinted with permission from [95] Copyright 2017, WILEY. (b) Comparison of electrode adhesion before and after PPy nanowires modification. Reprinted with permission from [95] Copyright 2017, WILEY. (c) Schematic diagram of ECoG drug delivery device for treating epilepsy. Reprinted with permission from [8] Copyright 2016, Elsevier.

Open Access Article. Published on 12 November 2024. Downloaded on 11/23/2024 4:14:03 AM.
This article is licensed under a Creative Commons Attribution 3.0 Unported Licence.

Journal of Materials Chemistry B Accepted Manuscript

View Article Online
DOI: 10.1039/D4TB02090A

Figure 8a shows the impedance test results of PPy thin-film electrodes and Au thin-film electrodes with the same geometric surface area. In comparison, the impedance of PPy films with the same surface area is smaller than 100Hz. PPy not only has good conductivity, but also biocompatibility, and is widely used in the preparation of ECoG electrodes. Petr et al. Purposed that iron(III) chloride is the oxidant of first choice in the preparation of PPy, and displays its biocompatibility from long-term experience, they compared the two forms of PPy, salt and alkali, and found that both had lower cytotoxicity, while the alkaline form of PPy had lower cytotoxicity (Figure 8b).[79] Almira et al. pointed out in 2007 that PPy did not detect cytotoxicity in mouse peritoneal cells[111], making it an attractive material for biomedical applications *in-vivo*.[112] For example, PPy can be applied to delivery devices for epilepsy treatment drugs.[8] Although PPy has its advantages, there is currently a problem of decreased conductivity due to peroxidation, which limits its long-term use.[113]

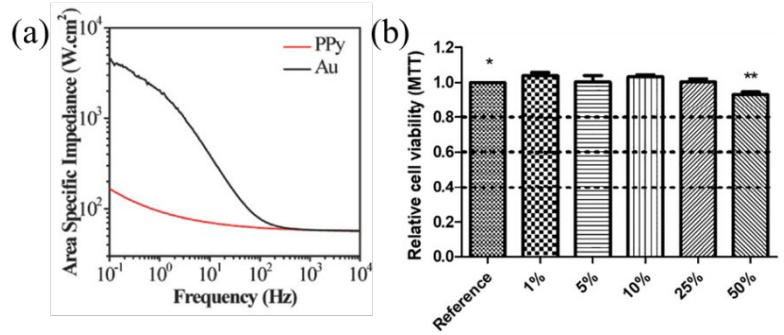

Figure 8. (a) Impedance compared with PPy film and Au film. Reprinted with permission from [95] Copyright 2017, WILEY. (b) Cytotoxicity of extracts of PPy towards NIH/3T3 cells compared to the reference. Reprinted with permission from [79] Copyright 2018, Elsevier.

Open Access Article. Published on 12 November 2024. Downloaded on 11/23/2024 4:14:03 AM.
This article is licensed under a Creative Commons Attribution 3.0 Unported Licence.

Journal of Materials Chemistry B Accepted Manuscript

View Article Online
DOI: 10.1039/D4TB02090A

Open Access Article. Published on 12 November 2024. Downloaded on 11/23/2024 4:14:03 AM.
This article is licensed under a Creative Commons Attribution 3.0 Unported Licence.

Journal of Materials Chemistry B Accepted Manuscript

3.2 Structural materials

Ensuring as good as possible conformal properties of the electrode upon tissue contact has long been a pursuit in the development of flexible ECoG thin-film electrodes.[114] The flexibility of the substrate directly impacts the overall flexibility of the electrode. Commonly employed flexible polymer materials for electrodes encompass PDMS, PI, parylene, and LCP. Over the recent years, the selection of patches for ECoG thin-film electrodes has expanded beyond individual polymer materials, with the emergence of composite structures that combine PDMS and parylene flexible films. This multilayer structure exhibits multiple advantageous properties that collectively enhance its ability to adapt to the intricate brain environment.

3.2.1 Polydimethylsiloxane

PDMS is a silicone-based elastomer[115] which have flexibility,[40, 42] processability,[37] biocompatibility,[39, 116, 117] corrosion resistance[118] and transparency,[31, 119] and it is frequently used as substrate materials for flexible electrode, such as carbon nanotube array (CNTA) can be transported to PDMS through chemical vapor deposition (CVD) to achieve electrode flexibility.[41] Chou et al. displayed a significantly curled PDMS electrode,[38] but the single-layer PDMS substrate has poor adhesion to most metal materials and is difficult to precipitate metal interconnects on the surface. Therefore, the electrode array, enclosed in a double-layer (DL) PDMS setup for gold interconnects as an insulation layer, shows good biocompatibility.[42] The

View Article Online
DOI: 10.1039/D4TB02090A

Open Access Article. Published on 12 November 2024. Downloaded on 11/23/2024 4:14:03 AM.
This article is licensed under a Creative Commons Attribution 3.0 Unported Licence.

Journal of Materials Chemistry B Accepted Manuscript

double-layer membrane structure permits the utilization of materials with distinct functionalities in each layer.[120] In recent years, the adhesion of flexible structure to metal electrode materials has been improved by combining PDMS and parylene materials. In **Figure 9a**, a flexible transparent electrode employs PDMS as a pliable substrate, wrapped with Cr/Au electrodes through a parylene interlayer and finally reduced impedance through PEDOT:PSS and MWCNTs material at the contact site between the electrode and the skin. It is considered advantageous that this electrode strategically employs diverse functional polymer materials across distinct structures, resulting in an average impedance of 20.2 ± 7.9 kΩ.[31] Similarly, Ochoa et al. chose PDMS (100~200 μm in thickness) be their flexible structure material and make ECoG electrode confirm the conformal coverage of the electrode over a curvature of 1 cm^{-1}. [40] Similarly, Vargo et al. shows an electrode that produced by PDMS can stably record ECoG signals.[43]

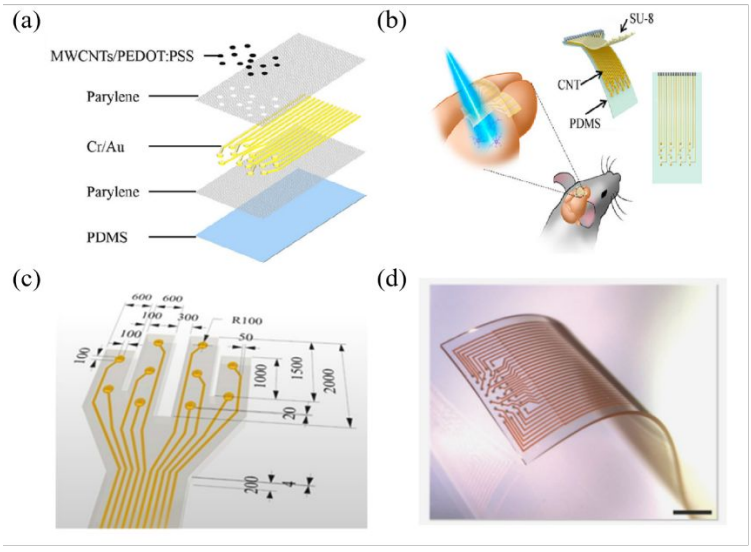

Figure 9. (a) A schematic diagram of the electrode structure configuration using a two-layer parylene encapsulated metal electrode, PDMS as a flexible substrate and PEDOT:PSS as a

View Article Online
DOI: 10.1039/D4TB02090A

contact coating. Reprinted with permission from [31] Copyright 2021, American Chemical Society. (b) Schematics of stretchable transparent CNT electrode array. Reprinted with permission from [121] Copyright 2018, American Chemical Society. (c) Multichannel ECoG electrode for mixed PDMS-parylene C. Reprinted with permission from [122] Copyright 2022, Elsevier. (d) Stretchable 32 channel electrode on PDMS substrate (Scale bar, 1 mm). Reprinted with permission from [122] Copyright 2022, Elsevier.

The performance testing of PDMS focuses on mechanical properties, including finite element analysis,[42] mechanical cycling testing and repeated extrusion testing. Zhao et al. fabricated a five-layer gold film structure electrode (green) with PDMS substrate and interlayer connection through Au nanopillars and compared its stretchability with single-layer gold film electrode (black) and double-layer gold film electrode (red) (**Figure 10a**, **10b**).[37] The stretchability of the single-layer electrode measured 80%, and for the double-layer electrode measured 120%, while the stretchability of the five-layer electrode reached 140%. Importantly, its resistance remained stable even after undergoing extensive cyclic testing. Chou et al. demonstrates the capability to execute a continuous bending cycle on the thin film, ranging from 0° to 180° and then returning to 0° at a rate of one cycle per second. Additionally, the bending cycles are performed on two distinct electrodes with varying traces, revealing no notable resistance alterations in either of the electrodes.[38] The electrode remains mechanically intact after undergoing 200000 bending cycles. Li et al. used a compression-based technique to measure the average electrode phase change resulting

Open Access Article. Published on 12 November 2024. Downloaded on 11/23/2024 4:14:03 AM.
This article is licensed under a Creative Commons Attribution 3.0 Unported Licence.

Journal of Materials Chemistry B Accepted Manuscript

View Article Online
DOI: 10.1039/D4TB02090A

from 100 and 1000 presses was −18.3 ± 4.9° and −19.1 ± 4.2°, the impedance values were 20.5 ± 2.1 kΩ and 20.0 ± 1.6 kΩ when they at 1 Hz (Figure 10c).[31] Of course, mechanical stretching can also affect the optical properties of thin films. Zhang et al. found that at a 20% stretching degree, the transmittance of CNT/PDMS electrode is higher than that of non-stretching (Figure 10d).[121]

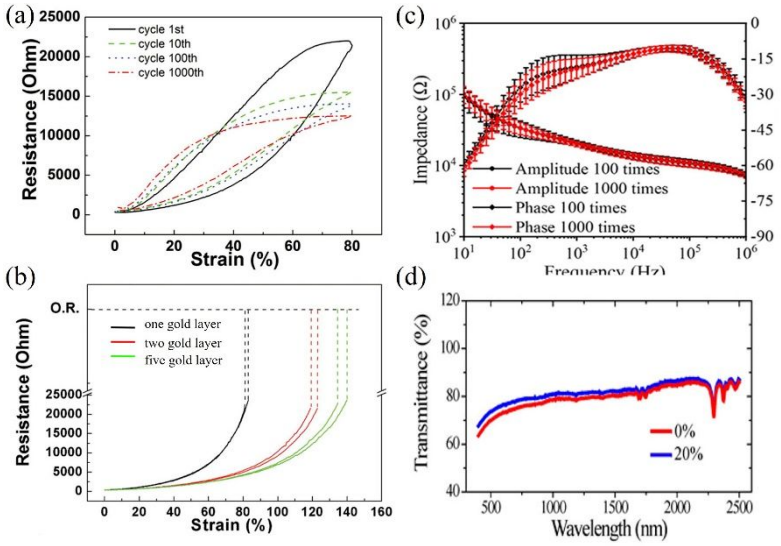

Figure 10. (a) The stretchability of the five-layer structure electrodes, reaching 140% compared to 80% for original one-layer electrodes and 120% for double-layered electrodes.[37] (b) The resistance-strain curve of the five-layer electrodes after 1, 10, 100, and 1000 stretching cycles, indicating the stability of the electrode after prolonged stretching cycles.[37] (c) Impedance of electrodes after pressing 100 and 1000 times. Reprinted with permission from [31] Copyright 2021, American Chemical Society. (d) Optical transmittance of a CNT/PDMS complex before stretching and under stretching to a strain of 20%. Reprinted with permission from [121] Copyright 2018, American Chemical Society.

Open Access Article. Published on 12 November 2024. Downloaded on 11/23/2024 4:14:03 AM.
This article is licensed under a Creative Commons Attribution 3.0 Unported Licence.

Journal of Materials Chemistry B Accepted Manuscript

View Article Online
DOI: 10.1039/D4TB02090A

Open Access Article. Published on 12 November 2024. Downloaded on 11/23/2024 4:14:03 AM.
This article is licensed under a Creative Commons Attribution 3.0 Unported Licence.

Journal of Materials Chemistry B Accepted Manuscript

3.2.2 Parylene

Parylene materials exhibit good metal adhesion, biocompatibility, processability and transparency.[123] Thin films of flexible array patches are frequently fabricated using chemical vapor deposition (CVD)[123], serving as adhesive and protective layers for metal electrodes.[124] The four common parylene variants[125] include: parylene C, parylene N, parylene D and parylene HT. Among these, parylene HT stands out with high temperature resistance (about 350 ℃),[50] facilitating the creation of continuous structures and exhibiting outstanding conformal properties. Transparent electrodes suitable for ECoG signal recording and two-photon Ca^{2+} imaging can be fabricated through sputter-deposition of ITO.[50] Parylene C has excellent electrical performance and is widely used in commercial electrodes. **Figure 11a** shows the flexible ECoG electrode made of parylene C substrate material and demonstrates its good curling flexibility.[55] Parylene not only exhibits good flexibility, but also demonstrates biocompatibility, making it a common choice for encapsulating metal electrodes.[38]

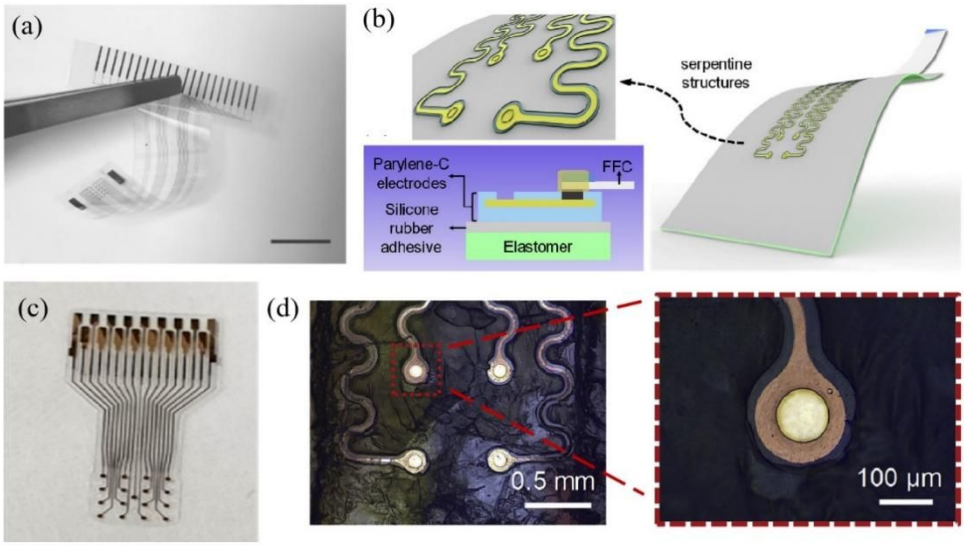

Figure 11. (a) The flexibility of an ECoG electrode prepared using parylene C as a

View Article Online
DOI: 10.1039/D4TB02090A

substrate. Reprinted with permission from [55] Copyright 2022, MDPI. (c) A parylene C coated electrode that has been stable for up to 56 days (equivalent to 115 days) in life testing. Reprinted with permission from [51] Copyright 2022, Elsevier. (b and d) Schematic diagram and micrograph of a serpentine structure. (left 0.5 mm, right 100 μm) Reprinted with permission from [32] Copyright 2019, Elsevier.

In terms of mechanical properties, parylene exhibits a lower Young's modulus. Yang et al. find the Young's modulus of parylene C film, determined through cyclic nanoindentation testing, remains relatively constant at approximately 4 GPa.[49] In **Figure12 a**, Setogawa et al. calculated bending stiffness of the device with and without the metal wiring layer as a function of the parylene thickness. Yamagiwa et al. presents the variation of deflection conducted on substrates composed of different thicknesses of parylene N and parylene C composites.[54] As the temperature gradually increases, the deflection of the substrate material continues to increase, displaying the favorable application scenarios of parylene materials in the field of flexible electrode substrates. Figure 12b, the resistance went up as the drop spacing increased. However, the growth rate of resistance on parylene is significantly lower than that on PDMS.[126] Moreover, parylene exhibits good electrical and optical properties. Choi et al. developed a parylene based ECoG electrode, with an average impedance range of 3.7 kΩ to 1.6 mΩ (1 kHz: 13.9 kΩ) (Figure 12c).[127]In addition, the parylene electrode sputtered with ITO has a transmittance of 80% in the visible light region of 450~750 nm.[52] Delamination is reported as one of the most common failure mechanisms of thin-film electrodes, and

Open Access Article. Published on 12 November 2024. Downloaded on 11/23/2024 4:14:03 AM.
This article is licensed under a Creative Commons Attribution 3.0 Unported Licence.

Journal of Materials Chemistry B Accepted Manuscript

View Article Online
DOI: 10.1039/D4TB02090A

the adhesion force between the electrode and the film determines the lifespan of the electrode.[128] Parylene materials have good adhesion performance in contrast to other polymer films, and peeling is commonly used to validate the adhesion strength of parylene to the electrode material. Nevertheless, this adhesion strength is susceptible to environmental factors. the peeling test was conducted following a 30 minute immersion in PBS, resulting in the detachment of some metals from the parylene film, indicating diminished adhesion of the parylene film to metals in humid conditions.[38] Kim et al. compared the silver wire printed on PDMS (blue) and transferred to a parylene film (red) as a function of drop spacing. In Kim et al. conducted lifetime tests on parylene electrodes, revealing the alterations in electrode impedance and channel count, as depicted in Figure 12d.[51] Within 13 days, the initial impedance increased from 14.2 kΩ to 40 kΩ (n = 16), After 13 days, the impedance of the electrode significantly decreased.

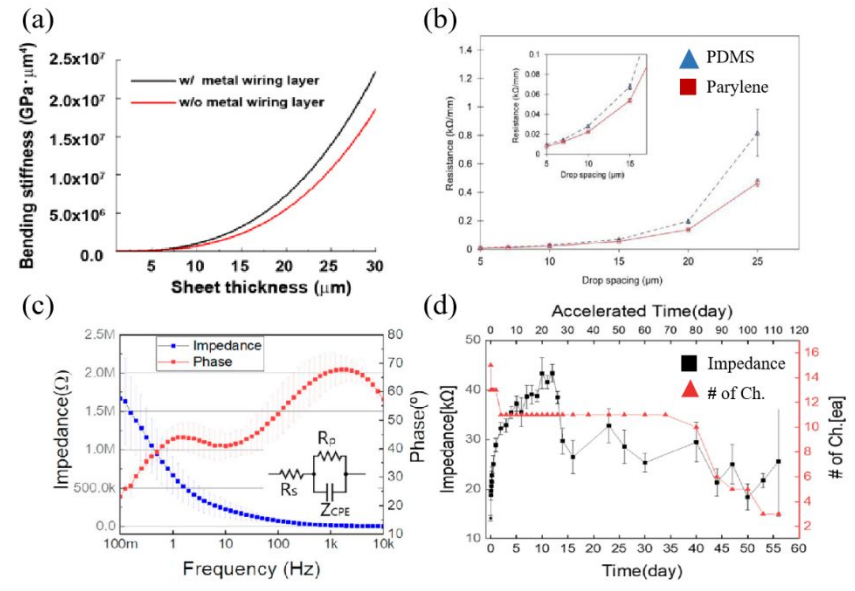

Figure 12. (a) Calculated bending stiffness of the device with and without the metal wiring layer as a function of the parylene thickness. Reprinted with permission from [129] Copyright 2023,

Open Access Article. Published on 12 November 2024. Downloaded on 11/23/2024 4:14:03 AM.
This article is licensed under a Creative Commons Attribution 3.0 Unported Licence.

Journal of Materials Chemistry B Accepted Manuscript

View Article Online
DOI: 10.1039/D4TB02090A

BMC. (b) Comparison of resistance between two electrode preparation methods. Reprinted with permission from [126] Copyright 2017, Elsevier. (c) Impedance and phase plots for the fabricated parylene C based ECoG electrodes. Reprinted with permission from [127] Copyright 2020, MDPI. (d) Plot shows the impedance variation and the number of alive channels during the lifetime test, reflecting the stability of the structure. Reprinted with permission from [51] Copyright 2022, Elsevier.

Open Access Article. Published on 12 November 2024. Downloaded on 11/23/2024 4:14:03 AM.
This article is licensed under a Creative Commons Attribution 3.0 Unported Licence.

3.2.3 Polyimide

PI material exhibits good biocompatibility, thermal stability, dynamic tensile strength and structural integrity.[115] It is suitable for insulation layers used in integrated circuits, active electronic devices and bioelectrodes through spin coating (**Figure 13a**).[34] Furthermore, PI displays good air permeability, which can prevent skin inflammation caused by long-term records. The primary role of the PI film is to passivate and protect the electrode structure. Figure 13b display manufacturing diagram is about a 32-channel conformal PI electrode, this electrode can conform to the curvature of the tissue and perfectly adhere to brain. Similarly, Figure 13c shows an insulating layer situated above the electrode, fabricated through the combination of capacitive $BaTiO_3$ and PI, with the resultant leakage current from this structure measuring only a few nanoamps.[67] The flexible gold film electrode is structured with a sandwich structure made of 5 μm PI.[98] PI material exhibits a certain flexibility. Vomero et al. manufactured a highly stable multi-layer thin-film electrode which is

Journal of Materials Chemistry B Accepted Manuscript

View Article Online
DOI: 10.1039/D4TB02090A

displayed by folding the 12-electrode glassy carbon array onto the PI substrate,[72] there is no significant change in impedance of this electrode before and after *in-vivo* and *in-vitro* testing. In comparison to other flexible materials, PI materials exhibit greater durability. Tolstosheeva et al. design a flex-rigid ECoG electrode, they chose PI as the substrate because it was considered to have better robustness at the same thickness.[130] Four years later, they prepared an ECoG electrode with waterproof properties that could maintain impedance stability in saltwater for 140 days (Figure 13d).[70]

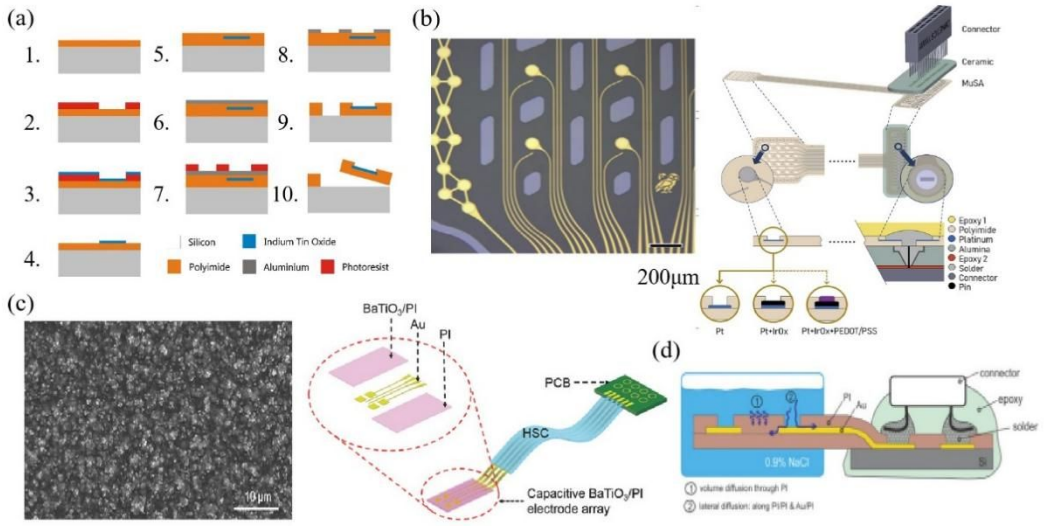

Figure 13. (a) Schematic of electrode preparation using PI as substrate. Reprinted with permission from [34] Copyright 2018, Elsevier. (b) The manufacturing diagram is about a 32-channel conformal PI electrode that can better fit the surface of the brain and bring the electrode closer to the signal source. The left image depicts the microscopic view of the electrode area, measuring 200 μm. Reprinted with permission from [23] Copyright 2017, Elsevier. (c) Electrode Array created by integrating capacitive $BaTiO_3$ and PI, with PI serving as an insulating protective layer.(The left image shows the SEM image of the prepared $BaTiO_3$/PI composite film, measuring 10 μm) Reprinted with permission from [67] Copyright 2017, WILEY. (d) The

Open Access Article. Published on 12 November 2024. Downloaded on 11/23/2024 4:14:03 AM.
This article is licensed under a Creative Commons Attribution 3.0 Unported Licence.

Journal of Materials Chemistry B Accepted Manuscript

View Article Online
DOI: 10.1039/D4TB02090A

electrodes encapsulated with PI are immersed in salt water, reflecting the good waterproof properties of PI. Reprinted with permission from [70] Copyright 2015, Elsevier.

PI is being focused on in terms of mechanical properties, Lin et al. investigated the alteration in conductor path resistance of the PI electrode under mechanical strain prior to fracture.[131] The electrode resistance exhibited an almost linear increase with the rising applied mechanical strain, and the tensile performance reached a threshold of 10%, which is sufficient for implantation applications. Xu et al. measured the Stress–strain curve and deformation force curve for PI films with thicknesses of 4 μm, 8 μm, 23 μm, and 50 μm. When the Young's modulus is similar, an increase in the thickness of the PI film leads to a corresponding rise in the ultimate tensile strength of the film.[132] When the electrode is placed in the brain environment, the stability of the electrode in the humoral environment and the conformability of the test determine the signal quality of the electrode, Tolstosheeva et al. compared the impedance changes of long-cured PI, short-cured PI and parylene in 170 days of body fluid testing and found that long-term cured PI has good impedance stability and is suitable as a high waterproof barrier (**Figure 14a** shows changes in impedance of long-cured PI). In Figure 14b, a Comsol model was employed to test the stress distribution in a PI electrode with dimensions of 4 μm, 10 μm and 20 μm within the cerebral cortex of rats (with L0 representing the working area where the electrode contacts the cortex, and L1 indicating the opposite end of the electrode), the force required for 10 μm electrode to fit the brain is much smaller than that required for 20 μm electrode. The miniaturization and lightweight development of the electrode can reduce the harm it brings to the subject.[23] In terms

Open Access Article. Published on 12 November 2024. Downloaded on 11/23/2024 4:14:03 AM.
This article is licensed under a Creative Commons Attribution 3.0 Unported Licence.

Journal of Materials Chemistry B Accepted Manuscript

View Article Online
DOI: 10.1039/D4TB02090A

of optical performance, Zátonyi et al. measured the optical transmission spectrum of PI/ITO/PI ECoG electrodes across wavelengths ranging from 400 nm to 720 nm. The transmittance throughout the entire wavelength range consistently remained at approximately 80% (Figure 14c), this reflects the good transmittance of PI.[34]

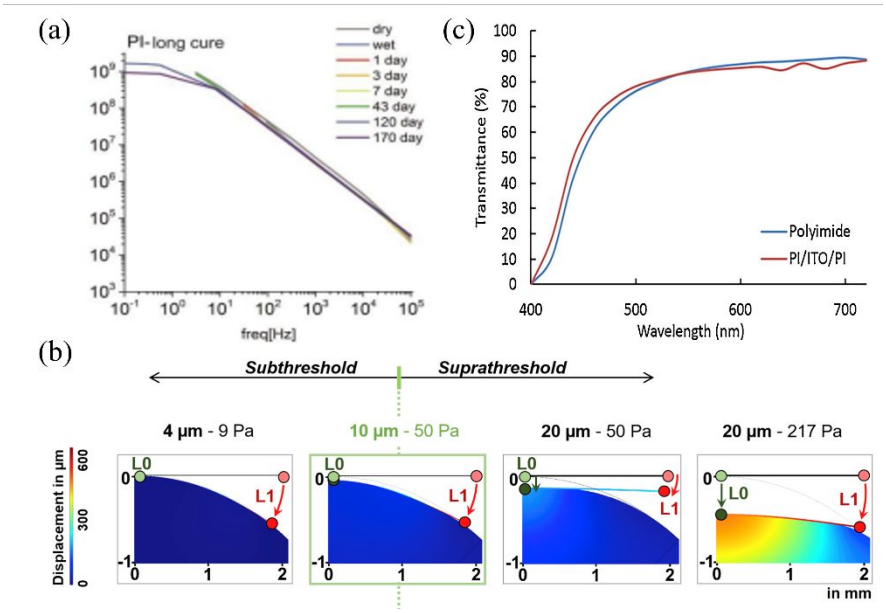

Figure 14. (a) Long term cured BPDA-PPD PI electrodes maintain stable impedance during long-term testing. Reprinted with permission from [70] Copyright 2015, Elsevier. (b) Finite element analysis images of electrodes with varying thicknesses under diverse forces on the cerebral cortex surface. Reprinted with permission from [23] Copyright 2020, Elsevier. (c) the Transmittance of PI/ITO/PI ECoG electrodes. Reprinted with permission from [34] Copyright 2018, Elsevier.

3.2.4 Liquid Crystal Polymer

The molecular chains of liquid crystal polymer (LCP) exhibit a one-dimensional

Open Access Article. Published on 12 November 2024. Downloaded on 11/23/2024 4:14:03 AM.
This article is licensed under a Creative Commons Attribution 3.0 Unported Licence.

Journal of Materials Chemistry B Accepted Manuscript

View Article Online
DOI: 10.1039/D4TB02090A

and two-dimensional long-range ordered arrangement in structure, exhibiting good flexibility, fluidity,[60] orientation and low water permeability. These characteristics are advantageous for prolonging the reliability and lifespan of implanted arrays. Moreover, LCP serves as self-adhesive thermoplastic material, facilitating the integration of multi-layer structures in thin-film electrodes.[133]

As shown in **Figure 15a**, it is a design of LCP electrode. Not only that, based on the improvement of electrode size, Chiang et al. designed five LCP thin-film electrodes based on thin-film technology, these electrodes can be applied to collect ECoG signals from rodents, non-human primates and humans according to different application scenarios.[133] Figure 15b shows the 25 channel neural electrodes with LCP substrate. Woods et al. compared the electrode lifespans of LCP and PI, illustrating that the LCP-encapsulated gold electrode outperforms the PI-encapsulated gold electrode in terms of longevity.[134] By predicting accelerated aging results, the device can maintain integrity for over 3.4 years. Mechanical property testing, Chiang et al. compared and analyzed the maximum bending force that commercial electrodes and LCP thin-film electrodes may exert on the brain from the four-point bending test and brain geometry analysis.[133] After that, Nicholas et al. calculated the effective flexural modulus of LCP film, LCP thin-film ECoG array, silicon, the bending force of silicon covered LCP, and commercial electrode, then they estimated the maximum force of these components could exert on the human brain, they fonund that LCP thin-film has a maximum pressure on the human brain that is only higher than LCP film, and the Young's modulus is within 10^{-1} GPa.[59] Michael, et al. tested the biocompatibility of LCP electrode, After

Open Access Article. Published on 12 November 2024. Downloaded on 11/23/2024 4:14:03 AM.
This article is licensed under a Creative Commons Attribution 3.0 Unported Licence.

Journal of Materials Chemistry B Accepted Manuscript

View Article Online
DOI: 10.1039/D4TB02090A

3 days and 28 days of recording, a comparison with the electrode experimental group revealed increased glial fibrillary acidic protein reactivity of astrocytes in the control group, whereas minimal increase was observed in astrocyte activation in the electrode experimental group, indicating the favorable biocompatibility of the LCP electrode. [135]

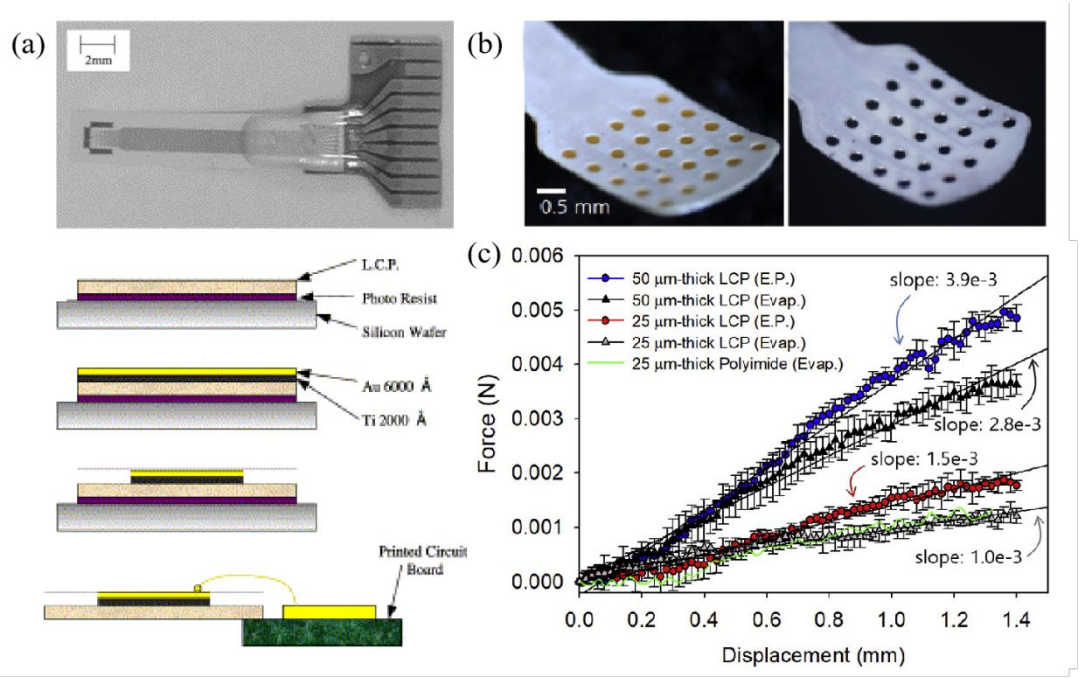

Figure 15. (a) The schematic and the fabrication process of a LCP electrode. Reprinted with permission from [136] Copyright 2004, Elsevier. (b) 25 channel neural electrode electroplated gold (left) or Iridium Oxide (right) based on LCP. Reprinted with permission from [137] Copyright 2019, Elsevier. (c) Bending force for LCP electrodes for electroplating (E.P.) and evaporation (Evap.), as well as flexibility comparison with PI electrodes. Reprinted with permission from [137] Copyright 2019, Elsevier.

4. Summary and Outlook

The polymer materials have been extensive used for ECoG thin-film electrodes.

Open Access Article. Published on 12 November 2024. Downloaded on 11/23/2024 4:14:03 AM.
This article is licensed under a Creative Commons Attribution 3.0 Unported Licence.

Journal of Materials Chemistry B Accepted Manuscript

View Article Online
DOI: 10.1039/D4TB02090A

Polymers such as PDMS provide flexibility to the structure of ECoG thin-film electrodes, while polymers such as PEDOT possess good conductivity to the ECoG thin-film electrodes. The method of enhancement of electrical properties of polymers is now focusing on minimizing impedance between brain tissue and electrodes. The application of conductive polymer coatings can further reduce the impedance compared to the uncoated electrodes. In terms of mechanical properties, flexible polymer materials have the Young's modulus more similar to brain tissue, providing greater comfort and less damage when placing the electrodes and making them easier to conform to the cerebral cortex. On this basis, the light transmittance of polymer materials can also provide a pathway for artificial regulation of brain activity through light stimulation. These aspects collectively underscore the merits of polymer-based ECoG thin-film electrodes.

However, the focus of ECoG thin-film electrodes is on how to detect high quality signals and avoid secondary damage. On one hand, many polymer materials for electrodes are used to reduce damage to brain tissue. On the other hand, subjecting individuals to craniotomies to remove the electrode after rescue or experiments can cause significant damage. If electrode materials could be engineered to undergo controlled degradation within tissue, the adverse effects of repetitive craniotomies could be averted. However, most currently available conductive polymers are not degradable. Natural polymers derived from organic sources present new perspectives; these materials exhibit good flexibility and biocompatibility, and even can be safely dissolved or absorbed by the body.[138, 139] Chitosan, for instance, offers antimicrobial

Open Access Article. Published on 12 November 2024. Downloaded on 11/23/2024 4:14:03 AM.
This article is licensed under a Creative Commons Attribution 3.0 Unported Licence.

Journal of Materials Chemistry B Accepted Manuscript

View Article Online
DOI: 10.1039/D4TB02090A

properties and modifiable conductivity; collagen provides a flexible and biocompatible matrix, while silk fibroin allows for tunable degradation rates. These polymers hold promise as potential materials for the next generation of ECoG thin-film electrodes. Furthermore, subjects often experience restricted mobility caused by the constraints of electrical wires connected to electrodes in long-term experiments with traditional ECoG electrodes.[140, 141] Wireless telemetry technology has brought about innovative solutions. By incorporating wireless telemetry modules onto thin film through strategic layering of various components, subjects can enjoy more freedom of movement during experiments. Despite facing numerous challenges, ECoG thin-film electrodes made of polymer materials continue to be widely utilized due to their exceptional properties.

Acknowledgements

This review was supported by the National Natural Science Foundation of China (52203309, 52373240), the Shanghai Sailing Program (22YF1400400), the Shanghai Rising-Star Program (23QA1400100), the Fundamental Research Funds for the Central Universities (2232022D-09), and the Open Fund of State Key Laboratory of Biobased Fiber Manufacturing Technology (SKL202317), Key-Area Research and Development Program of Guangdong Province (2023B0303030002). L. Y. acknowledges the financial support from the Shenzhen Science and Technology Program (Grant No. RCBS20221008093340100) and the funding supports of No. SE3Z007 and 52293425. S. S acknowledges support from the RGC Postdoctoral Fellowship Scheme (P0052633).

Conflict of Interest

The authors declare no conflict of interest.

Open Access Article. Published on 12 November 2024. Downloaded on 11/23/2024 4:14:03 AM.
This article is licensed under a Creative Commons Attribution 3.0 Unported Licence.

Journal of Materials Chemistry B Accepted Manuscript

View Article Online
DOI: 10.1039/D4TB02090A

References

[1] N. Wu, S. Wan, S. Su, H. Huang, G. Dou, L. Sun, *Infomat* **2021**, 3, 1174.

[2] X. Wang, X. Sun, D. Gan, M. Soubrier, H.-Y. Chiang, L. Yan, Y. Li, J. Li, S. Yu, Y. Xia, K. Wang, Q. Qin, X. Jiang, L. Han, T. Pan, C. Xie, X. Lu, *Matter* **2022**, 5, 1204.

[3] L. Wang, S. Liu, W. Zhao, J. Li, H. Zeng, S. Kang, X. Sheng, L. Wang, Y. Fan, L. Yin, *Advanced Healthcare Materials* **2024**, n/a, 2303316.

[4] A. Yu, M. Zhu, C. Chen, Y. Li, H. Cui, S. Liu, Q. Zhao, *Advanced Healthcare Materials* **2024**, 13, 2302460.

[5] N.-I. Kim, J. Chen, W. Wang, J. Y. Kim, M.-K. Kwon, M. Moradnia, S. Pouladi, J.-H. Ryou, *Advanced Healthcare Materials* **2024**, n/a, 2303581.

[6] H. Liu, X. Yuan, T. Liu, W. Zhang, H. Dong, Z. Chu, *Advanced Healthcare Materials* **2024**, n/a, 2304355.

[7] X. Wang, X. Xiao, Z. Feng, Y. Wu, J. Yang, J. Chen, *Advanced Healthcare Materials* **2023**, n/a, 2303479.

[8] R. Muller, Z. Yue, S. Ahmadi, W. Ng, W. M. Grosse, M. J. Cook, G. G. Wallace, S. E. Moulton, *Sensors and Actuators B: Chemical* **2016**, 236, 732.

[9] R. Balint, N. J. Cassidy, S. H. Cartmell, *Acta Biomaterialia* **2014**, 10, 2341.

[10] I. Tubia, M. Mujika, J. Artieda, M. Valencia, S. Arana, *Sensors and Actuators A: Physical* **2016**, 251, 241.

[11] G. Chen, D. Dang, C. Zhang, L. Qin, T. Yan, W. Wang, W. Liang, *Soft Matter* **2024**, 20, 7993.

[12] L. Sifringer, L. De Windt, S. Bernhard, G. Amos, B. Clément, J. Duru, M. W. Tibbitt, C. M. Tringides, *Journal of Materials Chemistry B* **2024**, 12, 10272.

[13] H. Dawit, Y. Zhao, J. Wang, R. Pei, *Biomaterials Science* **2024**, 12, 2786.

[14] M. E. E. Alahi, Y. Liu, Z. Xu, H. Wang, T. Wu, S. C. Mukhopadhyay, *Materials Today Communications* **2021**, 29, 102853.

[15] Q. Zeng, Z. Huang, *Advanced Functional Materials* **2023**, 33, 2301223.

[16] D. H. Szarowski, M. D. Andersen, S. Retterer, A. J. Spence, M. Isaacson, H. G. Craighead, J. N. Turner, W. Shain, *Brain Research* **2003**, 983, 23.

[17] M. Jorfi, J. L. Skousen, C. Weder, J. R. Capadona, *Journal of Neural Engineering* **2015**, 12, 011001.

[18] H. Wunderlich, K. L. Kozielski, *Current Opinion in Biotechnology* **2021**, 72, 29.

[19] J. Wang, T. He, C. Lee, *Nano Energy* **2019**, 65, 104039.

[20] N. Sharafkhani, A. Z. Kouzani, S. D. Adams, J. M. Long, G. Lissorgues, L. Rousseau, J. O. Orwa, *Journal of Neuroscience Methods* **2022**, 365, 109388.

[21] G. Buzsáki, C. A. Anastassiou, C. Koch, *Nature Reviews Neuroscience* **2012**, 13, 407.

[22] Y. Shi, R. Liu, L. He, H. Feng, Y. Li, Z. Li, *Smart Materials in Medicine* **2020**, 1, 131.

[23] M. Vomero, M. F. Porto Cruz, E. Zucchini, F. Ciarpella, E. Delfino, S. Carli, C. Boehler, M. Asplund, D. Ricci, L. Fadiga, T. Stieglitz, *Biomaterials* **2020**, 255, 120178.

[24] G. He, X. Dong, M. Qi, *Materials Research Express* **2020**, 7, 102001.

[25] A. Zatonyi, F. Fedor, Z. Borhegyi, Z. Fekete, *Journal of Neural Engineering* **2018**, 15, 054003.

[26] M. McDonald, D. Sebinger, L. Brauns, L. Gonzalez-Cano, Y. Menuchin-Lasowski, M. Mierzejewski, O.-E. Psathaki, A. Stumpf, J. Wickham, T. Rauen, H. Schöler, P. D. Jones, *Biosensors and Bioelectronics* **2023**, 228, 115223.

[27] X. Wei, L. Luan, Z. Zhao, X. Li, H. Zhu, O. Potnis, C. Xie, *Advanced Science* **2018**, 5, 1700625.

Open Access Article. Published on 12 November 2024. Downloaded on 11/23/2024 4:14:03 AM.
This article is licensed under a Creative Commons Attribution 3.0 Unported Licence.

Journal of Materials Chemistry B Accepted Manuscript

View Article Online
DOI: 10.1039/D4TB02090A

[28] A. B. Rapeaux, T. G. Constandinou, *Current Opinion in Biotechnology* **2021**, 72, 102.
[29] C. Rinoldi, Y. Ziai, S. S. Zargarian, P. Nakielski, K. Zembrzycki, M. A. Haghighat Bayan, A. B. Zakrzewska, R. Fiorelli, M. Lanzi, A. Kostrzewska-Księżyk, R. Czajkowski, E. Kublik, L. Kaczmarek, F. Pierini, *ACS Applied Materials & Interfaces* **2023**, 15, 6283.
[30] X. Wang, M. Wang, H. Sheng, L. Zhu, J. Zhu, H. Zhang, Y. Liu, L. Zhan, X. Wang, J. Zhang, X. Wu, Z. Suo, W. Xi, H. Wang, *Biomaterials* **2022**, 281, 121352.
[31] X. Li, Y. Song, G. Xiao, E. He, J. Xie, Y. Dai, Y. Xing, Y. Wang, Y. Wang, S. Xu, M. Wang, T. H. Tao, X. Cai, *ACS applied bio materials* **2021**, 4, 8013.
[32] B. Ji, Z. Xie, W. Hong, C. Jiang, Z. Guo, L. Wang, X. Wang, B. Yang, J. Liu, *Journal of Materiomics* **2020**, 6, 330.
[33] S. Oribe, S. Yoshida, S. Kusama, S.-i. Osawa, A. Nakagawa, M. Iwasaki, T. Tominaga, M. Nishizawa, *Scientific Reports* **2019**, 9, 13379.
[34] A. Zátonyi, Z. Borhegyi, M. Srivastava, D. Cserpán, Z. Somogyvári, Z. Kisvárday, Z. Fekete, *Sensors and Actuators B: Chemical* **2018**, 273, 519.
[35] S. Dong, W. Chen, X. Wang, S. Zhang, K. Xu, X. Zheng, *Vacuum* **2017**, 140, 96.
[36] W. Chen, J. Lin, Z. Ye, X. Wang, J. Shen, B. Wang, *Materials Horizons* **2024**.
[37] Y. Zhao, C. Li, M. Yu, Z. Yu, *Apl Materials* **2019**, 7, 101104.
[38] N. Chou, S. Yoo, S. Kim, *Ieee Transactions on Neural Systems and Rehabilitation Engineering* **2013**, 21, 544.
[39] A. Blau, A. Murr, S. Wolff, E. Sernagor, P. Medini, G. Iurilli, C. Ziegler, F. Benfenati, *Biomaterials* **2011**, 32, 1778.
[40] M. Ochoa, P. Wei, A. J. Wolley, K. J. Otto, B. Ziaie, *Biomedical Microdevices* **2013**, 15, 437.
[41] H. Yang, Z. Qian, J. Wang, J. Feng, C. Tang, L. Wang, Y. Guo, Z. Liu, Y. Yang, K. Zhang, P. Chen, X. Sun, H. Peng, *Advanced Functional Materials* **2022**, 32, 2204794.
[42] L. Guo, G. S. Guvanasen, X. Liu, C. Tuthill, T. R. Nichols, S. P. DeWeerth, *Ieee Transactions on Biomedical Circuits and Systems* **2013**, 7, 1.
[43] S. M. Vargo, T. Belloir, I. Kimukin, Z. Ahmed, D. J. Griggs, N. Stanis, A. Yazdan-Shahmorad, M. Chamanzar, presented at *2023 11th International IEEE/EMBS Conference on Neural Engineering (NER)*, 24-27 April 2023, **2023**.
[44] U.-J. Jeong, J. Lee, N. Chou, K. Kim, H. Shin, U. Chae, H.-Y. Yu, I.-J. Cho, *Lab on a Chip* **2021**, 21, 2383.
[45] B. Ji, M. Wang, C. Ge, Z. Xie, Z. Guo, W. Hong, X. Gu, L. Wang, Z. Yi, C. Jiang, B. Yang, X. Wang, X. Li, C. Li, J. Liu, *Biosensors and Bioelectronics* **2019**, 135, 181.
[46] W. Yang, Q. H. Fan, W. Li, presented at *2020 IEEE 15th International Conference on Nano/Micro Engineered and Molecular System (NEMS)*, 27-30 Sept. 2020, **2020**.
[47] T. J. Richner, S. Thongpang, S. K. Brodnick, A. A. Schendel, R. W. Falk, L. A. Krugner-Higby, R. Pashaie, J. C. Williams, *Journal of Neural Engineering* **2014**, 11, 016010.
[48] W. R. Lee, C. Im, C. S. Koh, J. M. Kim, H. C. Shin, J. M. Seo, presented at *2017 39th Annual International Conference of the IEEE Engineering in Medicine and Biology Society (EMBC)*, 11-15 July 2017, **2017**.
[49] W. Yang, Y. Gong, C.-Y. Yao, M. Shrestha, Y. Jia, Z. Qiu, Q. H. Fan, A. Weber, W. Li, *Lab on a Chip* **2021**, 21, 1096.
[50] A. Zatonyi, M. Madarasz, A. Szabo, T. Lorincz, R. Hodovan, B. Rozsa, Z. Fekete, *Journal of Neural Engineering* **2020**, 17, 016062.

Open Access Article. Published on 12 November 2024. Downloaded on 11/23/2024 4:14:03 AM.
This article is licensed under a Creative Commons Attribution 3.0 Unported Licence.

Journal of Materials Chemistry B Accepted Manuscript

View Article Online
DOI: 10.1039/D4TB02090A

[51] J.-H. Kim, D.-H. Baek, D. H. Kim, D.-W. Park, *Current Applied Physics* **2022**, 39, 214.
[52] K. Y. Kwon, B. Sirowatka, A. Weber, W. Li, *IEEE Transactions on Biomedical Circuits and Systems* **2013**, 7, 593.
[53] F. Vitale, W. Shen, N. Driscoll, J. C. Burrell, A. G. Richardson, O. Adewole, B. Murphy, A. Ananthakrishnan, H. Oh, T. Wang, T. H. Lucas, D. K. Cullen, M. G. Allen, B. Litt, *Plos One* **2018**, 13, e0206137.
[54] S. Yamagiwa, M. Ishida, T. Kawano, Ieee, presented at *26th IEEE International Conference on Micro Electro Mechanical Systems (MEMS)*, Taipei, TAIWAN, 2013
Jan 20-24, **2013**.
[55] Y. Kim, S. Alimperti, P. Choi, M. Noh, *Sensors* **2022**, 22, 1277.
[56] S. Shi, Y. Si, Y. Han, T. Wu, M. I. Iqbal, B. Fei, R. K. Y. Li, J. Hu, J. Qu, *Advanced Materials* **2022**, 34, 2107938.
[57] Y. Si, S. Shi, J. Hu, *Nano Today* **2023**, 48, 101723.
[58] Z. Yang, J. Zeng, Z. Yang, Y. Tong, Y. Lai, X. Cao, *Polymer* **2022**, 255, 125144.
[59] N. S. Witham, C. F. Reiche, T. Odell, K. Barth, C.-H. Chiang, C. Wang, A. Dubey, K. Wingel, S. Devore, D. Friedman, B. Pesaran, J. Viventi, F. Solzbacher, *Journal of Neural Engineering* **2022**, 19, 046041.
[60] R. Rihani, N. Tasnim, M. Javed, J. O. Usoro, T. M. D'Souza, T. H. Ware, J. J. Pancrazio, *Neuromodulation: Technology at the Neural Interface* **2022**, 25, 1259.
[61] L. Luan, J. T. Robinson, B. Aazhang, T. Chi, K. Yang, X. Li, H. Rathore, A. Singer, S. Yellapantula, Y. Fan, Z. Yu, C. Xie, *Neuron* **2020**, 108, 302.
[62] H. Moon, J. Kwon, J. Eun, C. K. Chung, J. S. Kim, N. Chou, S. Kim, *Advanced Materials Technologies* **2024**, 9, 2301692.
[63] E. Song, J. Li, S. M. Won, W. Bai, J. A. Rogers, *Nature Materials* **2020**, 19, 590.
[64] C. Sung, W. Jeon, K. S. Nam, Y. Kim, H. Butt, S. Park, *Journal of Materials Chemistry B* **2020**, 8, 6624.
[65] Y. Liu, V. R. Feig, Z. Bao, *Advanced Healthcare Materials* **2021**, 10, 2001916.
[66] I. B. Dimov, M. Moser, G. G. Malliaras, I. McCulloch, *Chemical Reviews* **2022**, 122, 4356.
[67] C. Chen, M. Xue, Y. Wen, G. Yao, Y. Cui, F. Liao, Z. Yan, L. Huang, S. A. Khan, M. Gao, T. Pan, H. Zhang, W. Jing, D. Guo, S. Zhang, H. Yao, X. Zhou, Q. Li, Y. Xia, Y. Lin, *Advanced Healthcare Materials* **2017**, 6, 1700305, 1700305.
[68] A. Schander, S. Strokov, H. Stemmann, T. Teßmann, A. K. Kreiter, W. Lang, *IEEE Sensors Journal* **2019**, 19, 820.
[69] E. Borda, D. I. Medagoda, M. J. I. A. Leccardi, E. G. Zollinger, D. Ghezzi, *Biomaterials* **2023**, 293, 121979.
[70] E. Tolstosheeva, V. Biefeld, W. Lang, *Procedia Engineering* **2015**, 120, 36.
[71] M. Vomero, E. Zucchini, E. Delfino, C. Gueli, N. C. Mondragon, S. Carli, L. Fadiga, T. Stieglitz, *Materials* **2018**, 11, 2486.
[72] M. Vomero, E. Castagnola, J. S. Ordonez, S. Carli, E. Zucchini, E. Maggiolini, C. Gueli, N. Goshi, L. Fadiga, D. Ricci, S. Kassegne, T. Stieglitz, presented at *2017 8th International IEEE/EMBS Conference on Neural Engineering (NER)*, 25-28 May 2017, **2017**.
[73] S. Carli, M. Bianchi, E. Zucchini, M. Di Lauro, M. Prato, M. Murgia, L. Fadiga, F. Biscarini, *Advanced Healthcare Materials* **2019**, 8, 1900765.
[74] P. D. Donaldson, Z. S. Navabi, R. E. Carter, S. M. L. Fausner, L. Ghanbari, T. J. Ebner, S. L. Swisher, S. B. Kodandaramaiah, *Advanced Healthcare Materials* **2022**, 11, 2200626.
[75] E. Castagnola, L. Maiolo, E. Maggiolini, A. Minotti, M. Marrani, F. Maita, A. Pecora, G. N. Angotzi,

Open Access Article. Published on 12 November 2024. Downloaded on 11/23/2024 4:14:03 AM.
This article is licensed under a Creative Commons Attribution 3.0 Unported Licence.

Journal of Materials Chemistry B Accepted Manuscript

View Article Online
DOI: 10.1039/D4TB02090A

A. Ansaldo, L. Fadiga, G. Fortunato, D. Ricci, presented at *2013 6th International IEEE/EMBS Conference on Neural Engineering (NER)*, 6-8 Nov. 2013, **2013**.

[76] D. Kumar, R. C. Sharma, *European Polymer Journal* **1998**, 34, 1053.

[77] D. Olvera, M. G. Monaghan, *Advanced Drug Delivery Reviews* **2021**, 170, 396.

[78] I. Fratoddi, I. Venditti, C. Cametti, M. V. Russo, *Sensors and Actuators B: Chemical* **2015**, 220, 534.

[79] P. Humpolíček, V. Kašpárková, J. Pacherník, J. Stejskal, P. Bober, Z. Capáková, K. A. Radaszkiewicz, I. Junkar, M. Lehocký, *Materials Science and Engineering: C* **2018**, 91, 303.

[80] S. Bhadra, D. Khastgir, N. K. Singha, J. H. Lee, *Progress in Polymer Science* **2009**, 34, 783.

[81] E. M. Geniès, A. Boyle, M. Lapkowski, C. Tsintavis, *Synthetic Metals* **1990**, 36, 139.

[82] M. A. Bhat, R. A. Rather, A. H. Shalla, *Synthetic Metals* **2021**, 273, 116709.

[83] K. R. Ryan, M. P. Down, N. J. Hurst, E. M. Keefe, C. E. Banks, *eScience* **2022**, 2, 365.

[84] L. Ouyang, C. Musumeci, M. J. Jafari, T. Ederth, O. Inganäs, *ACS Applied Materials & Interfaces* **2015**, 7, 19764.

[85] H. Aghazadeh, M. K. Yazdi, A. Kolahi, M. Yekani, P. Zarrintaj, J. D. Ramsey, M. R. Ganjali, F. J. Stadler, M. R. Saeb, M. Mozafari, *Current Applied Physics* **2021**, 27, 43.

[86] S. Manouchehri, B. Bagheri, S. H. Rad, M. N. Nezhad, Y. C. Kim, O. O. Park, M. Farokhi, M. Jouyandeh, M. R. Ganjali, M. K. Yazdi, P. Zarrintaj, M. R. Saeb, *Progress in Organic Coatings* **2019**, 131, 389.

[87] E. Castagnola, A. Ansaldo, E. Maggiolini, G. N. Angotzi, M. Skrap, D. Ricci, L. Fadiga, *Acs Nano* **2013**, 7, 3887.

[88] G. A. Woods, N. J. Rommelfanger, G. Hong, *Matter* **2020**, 3, 1087.

[89] S.-H. Sunwoo, S. I. Han, H. Joo, G. D. Cha, D. Kim, S. H. Choi, T. Hyeon, D.-H. Kim, *Matter* **2020**, 3, 1923.

[90] E. S. Boyden, F. Zhang, E. Bamberg, G. Nagel, K. Deisseroth, *Nature Neuroscience* **2005**, 8, 1263.

[91] Y. U. Cho, S. L. Lim, J.-H. Hong, K. J. Yu, *Npj Flexible Electronics* **2022**, 6, 53.

[92] A. Yazdan-Shahmorad, C. Diaz-Botia, Timothy L. Hanson, V. Kharazia, P. Ledochowitsch, Michel M. Maharbiz, Philip N. Sabes, *Neuron* **2016**, 89, 927.

[93] B. Janarthanan, C. Thirunavukkarasu, S. Maruthamuthu, M. A. Manthrammel, M. Shkir, S. AlFaify, M. Selvakumar, V. R. M. Reddy, C. Park, *Journal of Molecular Structure* **2021**, 1241, 130606.

[94] T. Araki, F. Yoshida, T. Uemura, Y. Noda, S. Yoshimoto, T. Kaiju, T. Suzuki, H. Hamanaka, K. Baba, H. Hayakawa, T. Yabumoto, H. Mochizuki, S. Kobayashi, M. Tanaka, M. Hirata, T. Sekitani, *Advanced Healthcare Materials* **2019**, 8, 1900130.

[95] D. Qi, Z. Liu, Y. Liu, Y. Jiang, W. R. Leow, M. Pal, S. Pan, H. Yang, Y. Wang, X. Zhang, J. Yu, B. Li, Z. Yu, W. Wang, X. Chen, *Advanced Materials* **2017**, 29, 1702800.

[96] M. J. Donahue, A. Sanchez-Sanchez, S. Inal, J. Qu, R. M. Owens, D. Mecerreyes, G. G. Malliaras, D. C. Martin, *Materials Science and Engineering: R: Reports* **2020**, 140, 100546.

[97] N. Rossetti, J. E. Hagler, P. Kateb, F. Cicoira, *Journal of Materials Chemistry C* **2021**, 9, 7243.

[98] S. Strokov, A. Schander, H. Stemmann, T. TeBmann, W. Lang, A. Kreiter, presented at *2017 IEEE SENSORS*, 29 Oct.-1 Nov. 2017, **2017**.

[99] E. Castagnola, L. Maiolo, E. Maggiolini, A. Minotti, M. Marrani, F. Maita, A. Pecora, G. N. Angotzi, A. Ansaldo, M. Boffini, L. Fadiga, G. Fortunato, D. Ricci, *IEEE Transactions on Neural Systems and Rehabilitation Engineering* **2015**, 23, 342.

[100] K. Gmucová, *Current Opinion in Electrochemistry* **2022**, 36, 101117.

[101] Z. Song, Y. Ma, A. Morrin, C. Ding, X. Luo, *TrAC Trends in Analytical Chemistry* **2021**, 135,

Open Access Article. Published on 12 November 2024. Downloaded on 11/23/2024 4:14:03 AM.
This article is licensed under a Creative Commons Attribution 3.0 Unported Licence.

Journal of Materials Chemistry B Accepted Manuscript

View Article Online
DOI: 10.1039/D4TB02090A

116155.

[102] P. Sakunpongpitiporn, K. Phasuksom, N. Paradee, A. Sirivat, *RSC Advances* **2019**, 9, 6363.

[103] Y. Hui, C. Bian, S. Xia, J. Tong, J. Wang, *Analytica Chimica Acta* **2018**, 1022, 1.

[104] P. Yadav, A. Patra, *Polymer Chemistry* **2020**, 11, 7275.

[105] N. Matsuhisa, X. Chen, Z. Bao, T. Someya, *Chemical Society Reviews* **2019**, 48, 2946.

[106] Y. Zhang, C. J. Sheehan, J. Zhai, G. Zou, H. Luo, J. Xiong, Y. T. Zhu, Q. X. Jia, *Advanced Materials* **2010**, 22, 3027.

[107] N. Nandihalli, C.-J. Liu, T. Mori, *Nano Energy* **2020**, 78, 105186.

[108] Y.-Z. Long, M.-M. Li, C. Gu, M. Wan, J.-L. Duvail, Z. Liu, Z. Fan, *Progress in Polymer Science* **2011**, 36, 1415.

[109] V. Raman, J.-E. Lee, H.-K. Kim, *Journal of Alloys and Compounds* **2022**, 903, 163799.

[110] S. Machida, S. Miyata, A. Techagumpuch, *Synthetic Metals* **1989**, 31, 311.

[111] A. Ramanaviciene, A. Kausaite, S. Tautkus, A. Ramanavicius, *Journal of Pharmacy and Pharmacology* **2007**, 59, 311.

[112] Y. O. Mezhuev, M. I. Shtil'man, A. A. Artyukhov, *Polymer Science, Series D* **2021**, 14, 427.

[113] I. Gablech, E. D. Głowacki, *Advanced Electronic Materials* **2023**, 9, 2300258.

[114] T. Cheng, Y. Zhang, W.-Y. Lai, W. Huang, *Advanced Materials* **2015**, 27, 3349.

[115] M. Xu, D. Obodo, V. K. Yadavalli, *Biosensors and Bioelectronics* **2019**, 124-125, 96.

[116] J. Liu, Y. Yao, X. Li, Z. Zhang, *Chemical Engineering Journal* **2021**, 408, 127262.

[117] D. Qi, K. Zhang, G. Tian, B. Jiang, Y. Huang, *Advanced Materials* **2021**, 33, 2003155.

[118] U. Eduok, O. Faye, J. Szpunar, *Progress in Organic Coatings* **2017**, 111, 124.

[119] M. P. Wolf, G. B. Salieb-Beugelaar, P. Hunziker, *Progress in Polymer Science* **2018**, 83, 97.

[120] Q.-C. Xia, M.-L. Liu, X.-L. Cao, Y. Wang, W. Xing, S.-P. Sun, *Journal of Membrane Science* **2018**, 562, 85.

[121] J. Zhang, X. Liu, W. Xu, W. Luo, M. Li, F. Chu, L. Xu, A. Cao, J. Guan, S. Tang, X. Duan, *Nano Letters* **2018**, 18, 2903.

[122] S. Bhaskara, T. Sakorikar, S. Chatterjee, K. V. Shabari Girishan, H. J. Pandya, *Sensing and Bio-Sensing Research* **2022**, 36, 100483.

[123] M. Golda-Cepa, K. Engvall, M. Hakkarainen, A. Kotarba, *Progress in Organic Coatings* **2020**, 140, 105493.

[124] T. Haggren, A. Shah, A. Autere, J.-P. Kakko, V. Dhaka, M. Kim, T. Huhtio, Z. Sun, H. Lipsanen, *Nano Research* **2017**, 10, 2657.

[125] Y. X. Kato, I. Saito, H. Takano, K. Mabuchi, T. Hoshino, *Neuroscience Letters* **2009**, 464, 26.

[126] Y. Kim, J. W. Kim, J. Kim, M. Noh, *Sensors and Actuators B: Chemical* **2017**, 238, 862.

[127] B.-J. Choi, J.-H. Kim, W.-J. Yang, D.-J. Han, J. Park, D.-W. Park, *Applied Sciences* **2020**, 10, 7364.

[128] P. Oldroyd, G. G. Malliaras, *Acta Biomaterialia* **2022**, 139, 65.

[129] S. Setogawa, R. Kanda, S. Tada, T. Hikima, Y. Saitoh, M. Ishikawa, S. Nakada, F. Seki, K. Hikishima, H. Matsumoto, K. Mizuseki, O. Fukayama, M. Osanai, H. Sekiguchi, N. Ohkawa, *Molecular Brain* **2023**, 16, 38.

[130] E. Tolstosheeva, V. Gordillo-González, T. Hertzberg, L. Kempen, I. Michels, A. Kreiter, W. Lang, presented at *2011 Annual International Conference of the IEEE Engineering in Medicine and Biology Society*, 30 Aug.-3 Sept. 2011, **2011**.

[131] J. H. Lin, Y. Wang, X. M. Wu, T. L. Ren, L. T. Liu, presented at *2009 2nd International Conference on Biomedical Engineering and Informatics*, 17-19 Oct. 2009, **2009**.

Open Access Article. Published on 12 November 2024. Downloaded on 11/23/2024 4:14:03 AM.
This article is licensed under a Creative Commons Attribution 3.0 Unported Licence.

Journal of Materials Chemistry B Accepted Manuscript

View Article Online
DOI: 10.1039/D4TB02090A

[132] F. Xu, Z. Zhou, H. Li, T. H. Tao, presented at *2021 IEEE 34th International Conference on Micro Electro Mechanical Systems (MEMS)*, 25-29 Jan. 2021, **2021**.

[133] C.-H. Chiang, C. Wang, K. Barth, S. Rahimpour, M. Trumpis, S. Duraivel, I. Rachinskiy, A. Dubey, K. E. Wingel, M. Wong, N. S. Witham, T. Odell, V. Woods, B. Bent, W. Doyle, D. Friedman, E. Bihler, C. F. Reiche, D. G. Southwell, M. M. Haglund, A. H. Friedman, S. P. Lad, S. Devore, O. Devinsky, F. Solzbacher, B. Pesaran, G. Cogan, J. Viventi, *Journal of Neural Engineering* **2021**, 18, 045009.

[134] V. Woods, M. Trumpis, B. Bent, K. Palopoli-Trojani, C.-H. Chiang, C. Wang, C. Yu, M. N. Insanally, R. C. Froemke, J. Viventi, *Journal of Neural Engineering* **2018**, 15, 066024.

[135] M. Schweigmann, L. C. Caudal, G. Stopper, A. Scheller, K. P. Koch, F. Kirchhoff, *Frontiers in Cellular Neuroscience* **2021**, 15, 720675.

[136] C. J. Lee, S. J. Oh, J. K. Song, S. J. Kim, *Materials Science and Engineering: C* **2004**, 24, 265.

[137] J. Jeong, K. S. Min, S. J. Kim, *Microelectronic Engineering* **2019**, 216, 111096.

[138] B. Basavaraju, S. Nagaraja, A. R. Banagar, C. V. Srinivasa, B. T. Ramesh, D. Ramdan, M. I. Ammarullah, *RSC Advances* **2024**, 14, 33332.

[139] S. Dehghan-Chenar, H. R. Zare, Z. Mohammadpour, *RSC Advances* **2024**, 14, 33301.

[140] C. Meng, D. Snizhko, Y. T. Zholudov, W. Zhang, Y. Guan, Y. Tian, G. Xu, *Chemical Communications* **2024**.

[141] F. Chen, X. Song, J. Fu, J. Liang, J. Zhou, J. Cai, Y. Zhang, M. Zhu, Y. Ding, J. Jiang, Z. Chen, Y. Qi, Z. Zhou, Q. Huang, Y. Zhang, Z. Zheng, *Journal of Materials Chemistry A* **2024**.

Open Access Article. Published on 12 November 2024. Downloaded on 11/23/2024 4:14:03 AM.
This article is licensed under a Creative Commons Attribution 3.0 Unported Licence.

Journal of Materials Chemistry B Accepted Manuscript

View Article Online
DOI: 10.1039/D4TB02090A

No primary research results, software or code have been included and no new data were generated or analysed as part of this review.

Open Access Article. Published on 12 November 2024. Downloaded on 11/23/2024 4:14:03 AM.
This article is licensed under a Creative Commons Attribution 3.0 Unported Licence.

Journal of Materials Chemistry B Accepted Manuscript